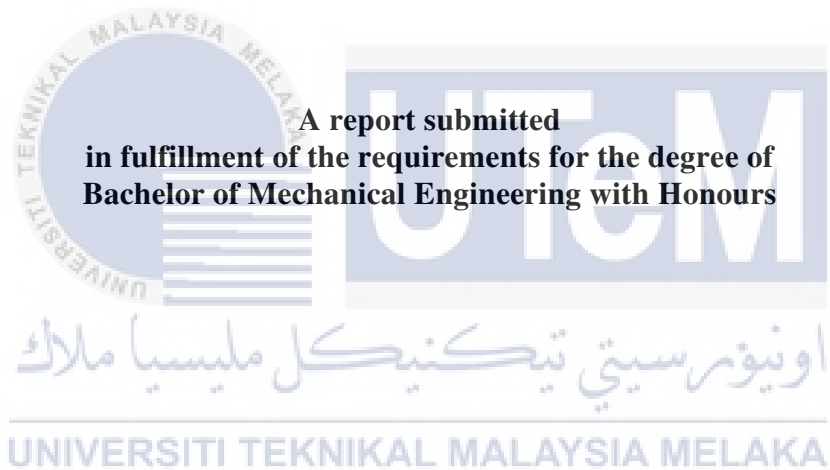# CFD STUDY ON THE IMPINGING JET VENTILATION TOWARDS INDOOR AIR QUALITY

LIM YIN CI

UNIVERSITI TEKNIKAL MALAYSIA MELAKA

CFD STUDY ON THE IMPINGING JET VENTILATION TOWARDS INDOOR AIR QUALITY

LIM YIN CI

A report submitted
in fulfillment of the requirements for the degree of
Bachelor of Mechanical Engineering with Honours

Faculty of Mechanical Engineering

UNIVERSITI TEKNIKAL MALAYSIA MELAKA

2021

DECLARATION

I declare that this project report entitled "CFD STUDY ON THE IMPINGING JET VENTILATION TOWARDS INDOOR AIR QUALITY" is the result of my own work except as cited in the references.

Signature : ....

Name : ....

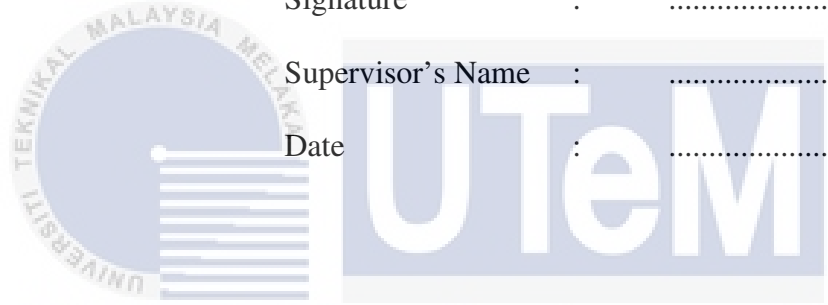Date : ....

APPROVAL

I hereby declare that I have read this project report and in my opinion this report is sufficient in terms of scope and quality for the award of the degree of Bachelor of Mechanical Engineering.

Signature   :   ....

Supervisor's Name   :   ....

Date   :   ....

ABSTRACT

The impinging jet ventilation system is a relative modern ventilation system which combine the positive effects from mixing and displacement ventilation. One of the demerits of this system is when for room cooling purpose, the cold supply air jet unable to distribute evenly in the room. The objective of this project is to develop a CFD model for impinging jet ventilation system and investigate the effects of position of exhaust and the shape of inlet toward the thermal condition and velocity field in a closed area. As the result, the position of exhaust brings a larger impact to the thermal condition in the test model while the shape of inlet shows a bigger influence in the velocity field in the test model when comparing to the position of exhaust. When placing the exhaust on the top of heat source, the heat generated can be remove more easily comparing to others location. Meanwhile by using a triangular inlet can lead to a higher inlet air velocity while maintaining a constant air flowrate. Finally, the recommendations for further research on the study of impinging jet ventilation system by using CFD are suggested such as run the simulation with ACT extension for thermal comfort so that the contour plots for mean age of air, PMV and PPD can be generate in the result tab.

i

ABSTRAK

Sistem pengudaraan jet pembantutan adalah sistem pengudaraan modern yang menggabungkan kesan positif daripada sistem pengudarran pencampuran dan anjakan. Salah satu demerit sistem ini ialah apabila guna dalam tujuan penyejukan bilik, jet udara bekalan sejuk tidak dapat mengedarkan jet udara ini secara sama rata di dalam bilik tersebut. Oleh itu tujuan projek ini adalah mengkaji beberapa aspek tentang sistem pengudaraan ini. Objektif projek tersebut adalah untuk membina model CFD untuk sistem pengudaraan tersebut dan menyiasat kesan-kesan tentang kedudukan ekzos dan bentuk salur masuk udara dengan keadaan terma dan medan halaju di dalam kawasan tertutup. Daripada hasil projek ini, didapati bahawa kedudukan ekzos membawa impak yang lebih besar kepada keadaan terma dalam model ujian manakala bentuk salur masuk menunjukkan pengaruh yang lebih besar dalam bidang medan halaju dalam model ujian. Apabila ekzos diletakkan di atas sumber haba, haba yang dihasilkan dapat dikeluarkan dengan lebih mudah berbanding dengan lokasi lain. Sementara itu dengan menggunakan bentuk salur masuk segi tiga dapat menjadikan halaju udara masuk tinggi manakala mengekalkan kadar aliran udara yang sama. Di dalam bahagian terakhir laporan ini, cadangan untuk penyelidikan lanjut mengenai kajian sistem pengudaraan tersebut dengan menggunakan CFD telah dicadangkan seperti menjalankan simulasi dengan sambungan ACT untuk keselesaan haba supaya plot kontur untuk umur min udara, PMV dan PPD boleh dijana dalam tab hasil.

ACKNOWLEDGEMENT

First and foremost, I would like to express my acknowledgement and sincere appreciation to my supervisor Dr. Mohamad Shukri Bin Zakaria from the Faculty of Mechanical Engineering in Universiti Teknikal Malaysia Melaka (UTeM). Dr provided a lot of guidance and help to me throughout this project. Through his constant supervision and ability to provide us with useful information for our project, I am able to complete the project successfully.

Moreover, I would also like to express my greatest gratitude to my seminar panel Ir. Dr. Nazri Bin Md Daud and Dr. Mohamad Firdaus Bin Sukri from Faculty of Mechanical Engineering. Their comment and advice on my project had point out the mistake that I made when constructing my report.

Last but not least, I would like to express my deepest gratitude to my peers, beloved parents and siblings. Their encouragement and moral support when the times got rough are much appreciated as it helped me to overcome the hard times.

TABLE OF CONTENT

LIST OF FIGURES

standing) and ceiling vicinity.

standing) and ceiling vicinity

LIST OF TABLES

LIST OF ABBREVIATIONS

HVAC – Heating, Ventilating and Air-Conditioning

IJV – Impinging Jet Ventilation

IAQ – Indoor Air Quality

CFD – Computational Fluid Dynamic

SBS – Sick Building Syndrome

ICOP on IAQ 2010 - Industry Code Of Practice On Indoor Air Quality 2010

DV – Displacement Ventilation

MV – Mixing Ventilation

DR – Draught rate/ Draft

PD – Percentage Dissatisfied

PMV – Predict Mean Vote

CIJV – Corner Impinging Jet Ventilation

ACE – Air Change Efficiency

ADPI – Air Distribution Performance Index
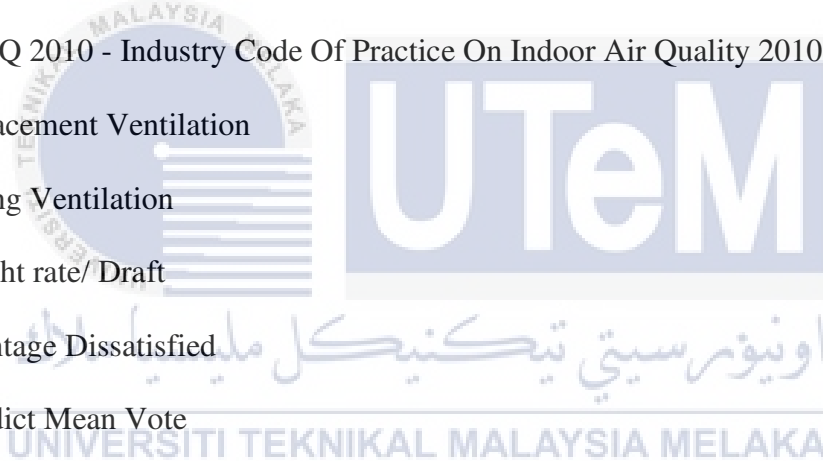
LIST OF SYMBOLS

H/d – jet to plate distance

S/d – jet-to-jet spacing

d – diameter

L – length

η - energy efficiency index

ε - contaminant removal efficiency

CHAPTER 1

INTRODUCTION

1.1   Background

In order to provide a preferable indoor thermal condition and air quality various types of heating, ventilating and air-conditioning (HVAC) system have been created and provide to the market. While in terms of ventilating system there are various types of mechanical ventilation system present which are mixing ventilation, displacement ventilation, impinging jet ventilation and confluent jet ventilation.

The key concept for a mixing ventilation system is to mix the fresh air outdoor with indoor air to dilute the emissions such as heat from indoor source. Normally, mixing ventilation system is design by having an air jet supplied at the ceiling or upper part of wall with air velocity equal or higher than 2 m/s to provide air jets circulation around the room. While in order to prevent high pressure accumulated inside the room an outlet for air flow is set at high level. Although the design is simply and easy, this mixing ventilation system still has its disadvantages which includes the uniform air velocity is high in working space and lead to a higher turbulence in the specific room and making the people inside feels discomfort. Besides that, mixing ventilation system has a low efficiency of ventilation this will causes high pollutant concentrations remain in the air for long periods.

Meanwhile for displacement ventilation system is a ventilation strategy that emerged in the 1970's. The key concept of this ventilation system is based on the principle of displacing indoor air with fresh air supplied from outside. Not like the mixing

1

ventilation system, this system having a low inlet air velocity which is around 0.5m/s and is supplied near the floor level. While the outlet is set at high level. This design will create an upward air flow inside the room, as the air flow through the heat sources in the room the cold air will absorb heat from the heat sources and create thermal plumes at the high level in the room. This situation will form a vertical gradient of air temperature which fits the concept of buoyancy and have a positive effect for the air ventilation. While the disadvantage of this design is also critical which is displacement ventilation has a limited penetration depth into the room which make this system less efficient in a large room.

Due to the shortcoming in the mixing ventilation and displacement ventilation system, new ventilating system are introduced which are impinging jet ventilation system and confluent jet ventilation system. These two types of ventilating system not only combine the positive outcome of mixing ventilation system and displacement ventilation system also solve the problems face by these two systems. As for impinging jet ventilation system, this system used a duct to supply air jet toward the floor and spread over the floor. Due the characteristic of a medium momentum air supply, the supplied air will cover a larger surface area compare to the displacement ventilation system. While for confluent jet ventilation, the supply air is not supply to the room through directly hit on the floor but using a closely spaced slots or circular apertures with same flow directions to supply a jet of air at the floor level of the room. This creates a similar effect to impinging jet ventilation system.

1.2   Problem Statement

The impinging jet ventilation (IJV) system is a relatively modern ventilation method that proposed in the late 1990's. Although this system holds the strength of mixing ventilation and displacement ventilation, it still has its own weakness. One of the demerits of this system when for room cooling purpose, the cold supply air jet unable to distribute evenly in the room. This situation will make the crowd who staying inside the room experience different thermal condition. The person who near to the nozzle of IJV system in the room will feel colder compare to those who far from it. Hence this report will carry out a study to improve the performance of impinging jet ventilation system so that the impinging jet ventilation system can evenly supply the air to all the places in a closed area compare to an investigation done by previous researcher using computational fluid dynamic (CFD).

1.3   Objective

The objectives of this study are:

i. To develop CFD model of impinging jet ventilation in a closed area.

ii. To analyse the effect of impinging jet with various nozzle and position of exhaust towards indoor air quality of a closed area.

1.4   Scope of study

The study for this project will be fully done by using the CFD software. The study will cover the investigation of previous case which had use IJV system as the mechanical ventilation system. Next in this study, the geometry and condition of the previous case will be reform and then by using the previous case as reference and this project will modify the IJV system in the previous case by changing nozzle size or height condition in order to achieve a better performance compare to the previous case.

3

CHAPTER 2

LITERATURE REVIEW

2.1   Indoor Air Quality

Indoor Air Quality (IAQ) is pointed to the air quality inside a building or structure. US Environmental Protection Agency (EPA, 2016) defines Indoor Air Quality (IAQ) as a quantitative variable which refers to the air quality within and around buildings and structures, especially as it relates to the health and comfort of building occupants." But due to lack of consistent metrics and standards, the measurement of IAQ is always vary depending on the perspectives for the person who planning to do this measurement. In general, measurement of IAQ for a building usually point to determine the percentage of pollutants found in the indoor air which include chemical pollutants, concentration of carbon monoxide, formaldehyde levels and others particular substance that can be dissolve in air. Next, IAQ also evaluate does the air condition inside the building is comfort and human friendly such as the thermal condition and humidity of the air around the building. (Anne Steinemann, et al, 2016)

The indoor air quality article at the official website of Department Of Occupational Safety And Health, Ministry of Human Resource has stated that a poor IAQ inside a workplace will make the person inside the building feeling discomfort and may lead to sick building syndrome (SBS). This situation will directly affect the productivity of the worker. Meanwhile a good IAQ not only will protect the health of the people inside the building but will also provide a pleasant and comfort environment.

2.1.1 Sick Building Syndrome

Sick Building Syndrome also known as SBS is an amalgamation of symptoms that due to various exposure on specific building conditions (Lu, et al, 2017). The name of this Sick Building Syndrome is come from the World Health Organization (WHO) where it is a collection of some common symptoms including itchy eyes, running nose and throat irritation, mental fatigue, headaches, nausea, dizziness and skin irritations, which mostly have relationship with environment of the individu. (Ghaffarianhoseini, et al, 2018; WHO 1983). Not like others well-defined building-related illnesses that can easily diagnosed, sick building syndrome is point to the situation in which building occupants experience ill health that appear to be linked to combination of several element in a particular building, hence the identification of illness or cause become very troublesome (Carrie A Redlich, et al, 1997). The rise of this SBS is due to the energy crisis in 1970's which make the air ventilation inside the indoor office decrease significantly. This condition has affected the rate of air change indoor per hour drop from 2 to 0.2 or 0.3 which lead to the fresh supply air for the building occupants drop to $5ft^3$/person from original 20-30 ft^3/ person (Mohammad Javad Jafari, et al, 2015; Hess-Kosa K., 2010).

2.1.2 Industry Code Of Practice On Indoor Air Quality 2010

Industry Code of Practice on Indoor Air Quality 2010 (ICOP on IAQ 2010) is a standard code of practice for industry that publish by Department of Occupational Safety and Health (DOSH). On 30 August 2010, Minister had approved this ICOP and replace the Code of Practice on Indoor Air Quality launched by the him on July 2005. The main purpose of this ICOP is to provide guidance on achieving better IAQ and to set minimum standard for some selected parameters which can avoid discomfort and adverse health effect among the person who most of the time staying inside an enclosed area which is equip with mechanical ventilating and air conditioning (MVAC) system including air-cooled split unit.

This ICOP applies to all type of buildings which are equip with MVAC system in Malaysia, except:

1. domestic buildings;
2. any area or any part of the building which is constructed, used or intended to be used for domestic or industrial purposes;
3. any area or part of building where any chemicals hazardous to health are used for analytical, research or preservation purposes; or
4. removal and disposal of asbestos containing materials.

Table 2.1 shows the parameters which normally will include in testing the indoor air quality of a building and their acceptable range in this industry code.

Table 2.1: IAQ Test Parameters and Acceptable Range or Limits (Department of

Occupational Safety and Health (DOSH), 2010)

No.	Test Parameter	Acceptable Range / Limit
Physical Parameter		
1.	Air Temperature	23 ° C - 26 ° C
2.	Relative Humidity	40 % - 70 %
3.	Air Movement	0.15 - 0.50 m/s
Chemical Contaminants		
4.	Carbon Monoxide (CO)	10 ppm
5.	Formaldehyde (CH_2O)	0.1 ppm
6.	Ozone (O_3)	0.05 ppm
7.	Respirable particulates (PM_{10})	0.150 mg/m^3
8.	Total volatile organic compounds ($TVOC_S$)	3.00 ppm
Biological Contaminants		
9.	Total Bacterial Counts	1000 cfu/m³
10.	Total Fungal Counts	500 cfu/m³
Ventilation Performance Indicator		
11.	Carbon Dioxide	Ceiling limit: 1000 ppm

Notes for Table 2.1:

a. For chemical contaminants, the limits are eight-hour time-weighted average airborne concentrations.

b. mg/m^3 is milligrams per cubic meter of air at 25° Celsius and one atmosphere pressure.

c. ppm is parts of vapour or gas per million parts of contaminated air by volume.

d. cfu/m^3 is colony forming units per cubic meter.

e. the ceiling limit shall not be exceeded at any time. Readings above 1000ppm are indication of inadequate ventilation.

f. excess of bacterial counts does not necessarily imply health risk but serve as an indicator for further investigation.

2.2   Impinging Jet

Impinging Jet is a strong technique to be used in various cooling situation such as maintaining working temperature for certain electronic components, reducing temperature for metal and glass tempering, cooling of gas turbine blades, paper drying, etc (G.J. Poitras, et al, 2017). Due to its high heat transfer coefficients properties, impinging jet cooling not only efficient in low heat load cooling but also a good cooling mechanism for high heat loads condition. (Julia Wienand, et al, 2016). The properties that make this impinging jet special from others jet is the flow field of impinging jet has several different flow properties. The flow field produced by impinging jet can be separate into three different region which are free-jet region, impingement region and wall-jet region (Figure 2.1). Where the d and h in the Figure 2.1 is the diameter of nozzle and the nozzle to plate distance. The free jet region can be further distinct into three zones depending on the distance between the nozzle and the plate perpendicular to the nozzle. These zones are the potential core zone, developing zone and fully developed zone (Figure 2.2).
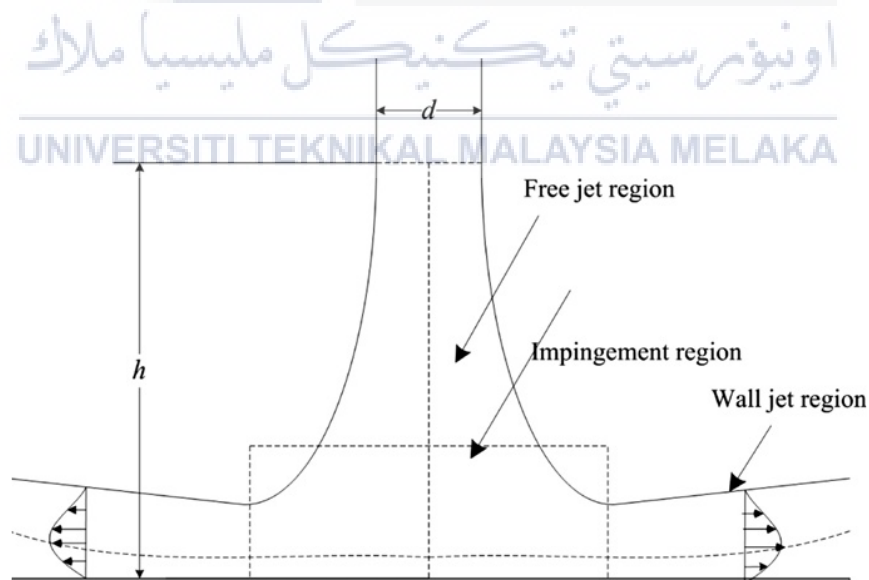
Figure 2.1: Flow regions of an impinging jet (Karimipanah, et al, 2002)

Initially the air jet pump out from the nozzle and the impulsive force on the air jet entrained the surrounding air to flow in the same direction with it thus reducing the

8

velocity of air jet. Where this situation forms a phenomenon that there is mixing and shear region surrounds a core of air jet at the centreline of the nozzle and we call this zone as potential core zone. In this zone, the centreline velocity of jet remains unchanged and the air jet is mostly in laminar flow properties. But the mean velocity at the shear layer is lower than the centreline velocity and the turbulence intensity is high at this layer. Typically, the range for this potential zone is around 6 to 7 diameters or slot widths downstream of the nozzle depending on exit conditions of the velocity and turbulence intensity. Furthermore, the range of this potential core zone will be reduced if the density of air jet is lower than the density of the surrounding air (Jambunathan et al., 1992).

In the developing zone, the air jet entrained more and more surrounding air and causing the region of the air jet become wider in spatial extent. The incoming surrounding air will interact with the air flow which originate pump out from the impinging jet device and makes the portion of air flow which having the initial velocity at centreline of jet become narrower. At the fully developed zone, the centre velocity of the air jet decreases rapidly due to interference of the surrounding air. In this region, air jet attains a self-similar behaviour and the mean velocity profile can be approximated with a Gaussian profile (Jambunathan et al., 1992).
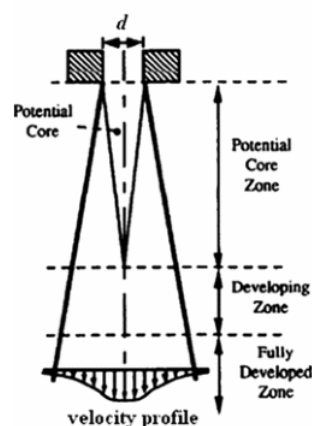
Figure 2.2: Further Distinction for Free Jet Region

As the air jet approaches to the wall, the air flow is deflected from the axial direction into radial direction and perform a disk shape spreading pattern to the surrounding while this region is known as the impingement region (Figure 2.3). The air at the centre of the disk shape spreading pattern is normally under stagnation condition where the local velocity of air at that point is nearly zero. The part of wall-normal velocity decreases rapidly, while the corresponding pressure rises rapidly. The high normal and shear stresses in the turning flow have a direct effect on the local transport properties (Zuckerman and Lior, 2006). For round jets, the impingement area usually extends 1.2 nozzle diameters above the wall (Martin, 1977). As it travels away from the nozzle, the turning flow expands radially outward parallel to the wall surface and thickens. This is referred to as the wall jet area (Karimipanah, et al, 2002).
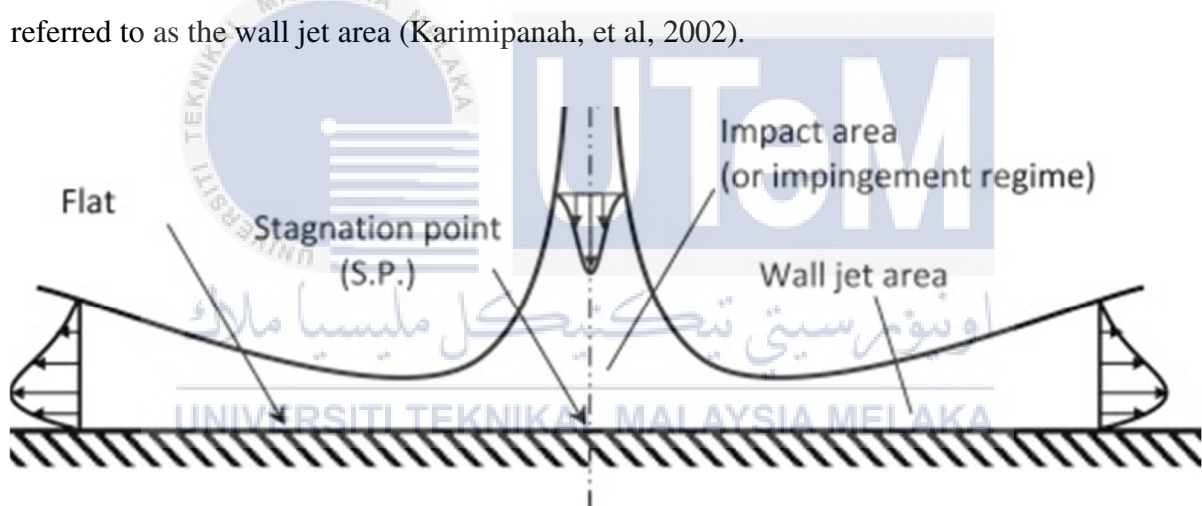
Figure 2.3: Impingement Region and Wall-Jet Region

From the study by Surendra D. Barewar, et al (2019) has proved that the jet to plate distance (H/D ratio) play an important role in the jet impingement cooling process and the concentration of coolant also has a huge effect on the cooling process especially at the stagnation zone. The study found out that by having a high concentration coolant jet will increase the cooling rate at the stagnation zone of impinging jet. P. Balakrishnan and K. Srinivasan (2019) did an experiment on the noise produce by various shape of impinging jet. They found out that noncircular jets mitigate or eliminate the impinging tones compared to the circular jet. Square jet is quieter at low nozzle pressure ratio and almost completely eliminate the supersonic impinging tones at higher under expansion conditions.

In a study by Uddin, et al (2019) has found out that the heat transfer rate in impinging jet system can be enhance by active excitation frequency. Meanwhile, the passive excitation of the jet by inserting inserts (Figure 2.4b) into the place near to the end of the flow tube, lead to a large decrease in pressure, while swirl (Figure 2.4c) does not always result in an appreciable increase in heat transfer rates.
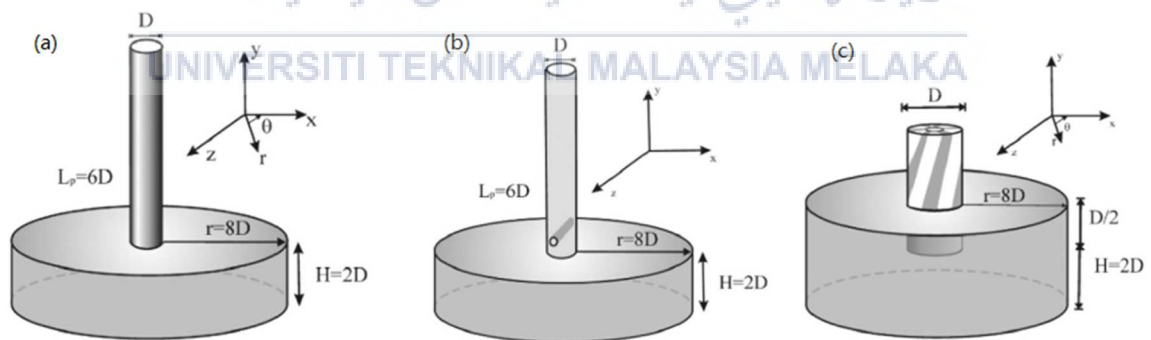
Figure 2.4: Schematic diagram of the computational domains used for different simulations (a) non-swirling non excited jet, (b) passively excited jet with cylindrical insert, (c) swirling jet. A swirling device is shown for clarification but is not modelled. (Uddin, et al, 2019)

From the study done by Bin Sun, et al (2016) has shown that by using nanofluids on impinging jet cooling systems can increase the heat transfer efficiency significantly without affecting the pressure drop in the system. Next, in their study also prove that the circular shape nozzle can perform better in cooling compare to square shape nozzle and the larger the jet angle to the plane the stronger the heat transfer effect where the ideal jet impingement cooling effect is meet at 90º jet angle. According to Makatar Wae-hayee, et al (2019), the highest average Nusselt number was found at jet-to-plate distance h/d = 4 for all jet-to-jet spacings (S/d) (Figure 2.5). While the secondary peak of the local Nusselt number can be found by having a large jet-to-jet spacing where S/d ≥ 6 combined with a short jet to-plate distance where H/d ≤ 4 and the Reynolds number of the flow is bigger than 30,000.

(a)

(b)
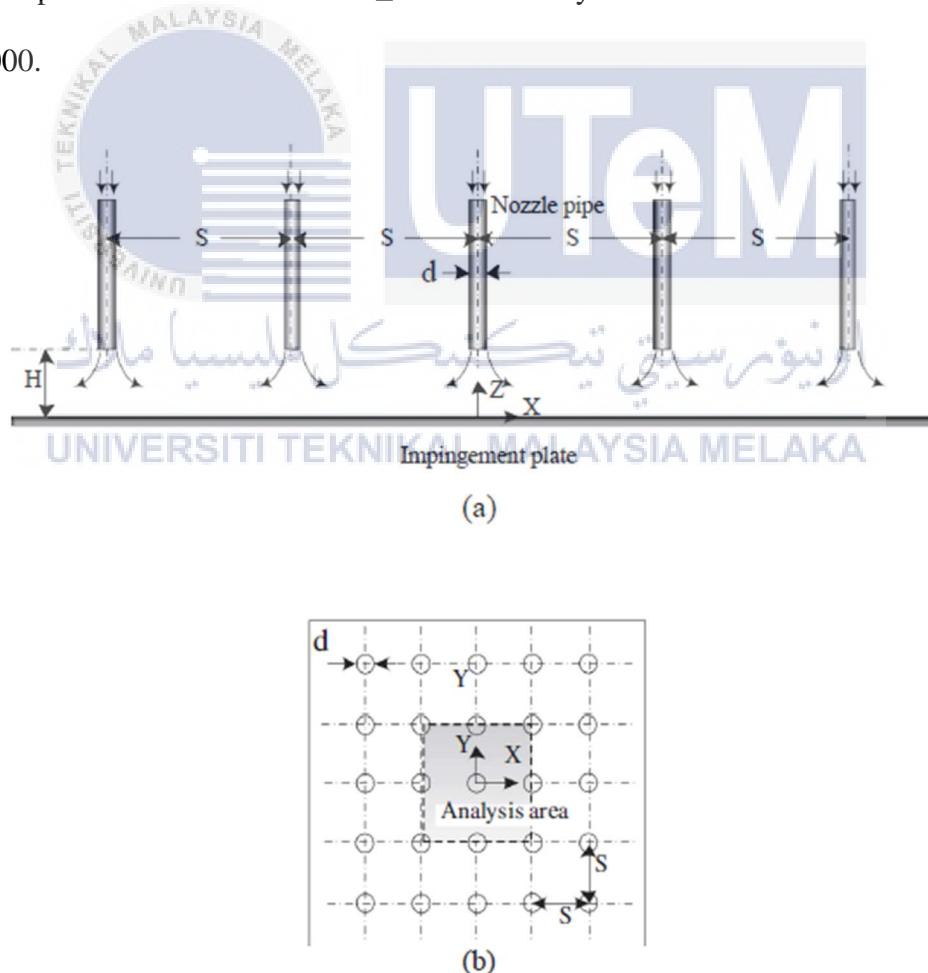
Figure 2.5: (a) Impinging jets from pipe nozzles and (b) Nozzle arrangement (Makatar Wae-hayee, et al, 2019)

The flow and heat transfer characteristics of an impinging jet from a pipe nozzle with an air-augmented duct were investigated by C. Nuntadusit et al (2018). The heat transfer rate on the impingement surface for an air-augmented duct (Figure 2.6b) is noticeably higher when the diameter of the air-augmented duct is between 2x and 4x of the inner diameter of the main pipe nozzle, d, and the length of the augmented duct, L, is equal to 2x of the inner diameter of the main pipe nozzle than for conventional impinging jets (Figure2.6a)
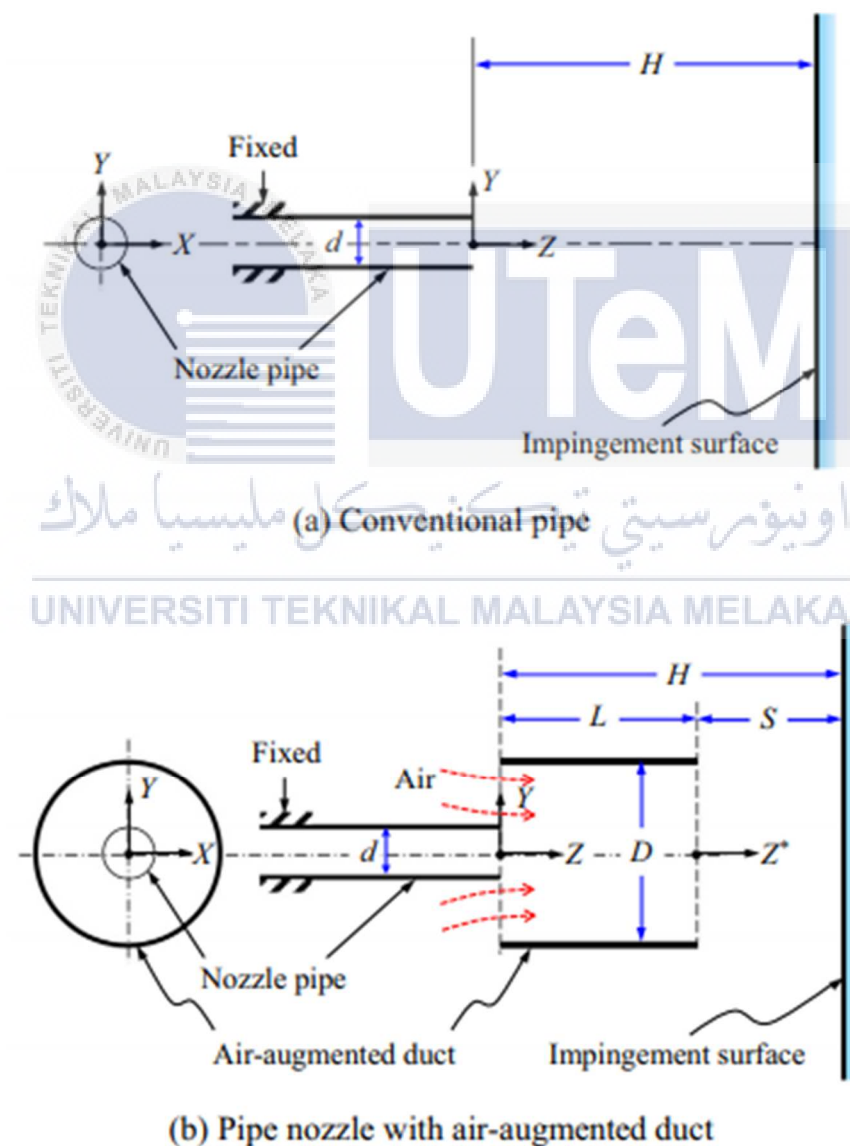
Figure 2.6: Detail for Conventional Pipe and Pipe Nozzle with Air-augmented Duct (C. Nuntadusit, et al, 2018)

2.3   Impinging Jet Ventilation

According to Ye, et al. (2019), impinging jet ventilation system (IJV) is a potential ventilation strategy which combines the merits of displacement ventilation (DV) and mixing ventilation (MV) while on the other hand overcomes the demerits of DV which is inefficient in room heating and MV which has a large working load. From the result of their study shown that there is a huge difference of the proportion of the supply air delivered to the breathing zone between IJV and MV due to the difference in the ways of introducing supply air into the targeted zone. The airflow pattern for IJV is a bottom-up flowing sequence. The air supply by the IJV will firstly spread a certain distance along the floor after it introduce to the room, then slowly separate from the floor and flows upwards to the ceiling. The supplied air jet mixes with the room air and perform a large recirculation zone covering most of the area of the ventilation room.

Where the airflow pattern for MV is more distorted and chaos. The supplied air by MV move into the room from ceiling level and the turbulence intensity of the flow become large after traveling few distance from the supply inlet. Due to the outlet for MV is also at high level, the air supply by MV unable to cover all space in the room. This makes mean age of air in the breathing zone for case IJV is 37–47% less than case MV. This statement indicates that the supply air enters and leaves the particular room for IJV system takes shorter time compare to MV system. Next, the numerical results also show that both of the carbon dioxide and 2.5 µm particles distribute uniformly in the case IJV for the constant volume (CAV) and variable volume (VAV) systems, while for case MV the CO2 mainly distributes in the middle region of the room height and the 2.5 µm particles concentrate at the floor level away from the exterior wall.

Another research by Ye, et al. (2018) has proved that the increasing rate of the heat loss of the room under a cold weather with an evident thermal stratification for MV is almost 2.4~4 times higher than that for IJV. While in terms of indoor air quality IJV system also shows a better result compared to MV while using lower ventilation energy requirement, meanwhile the performance of DV system generally similar with IJV system but its limitations on the amount of cooling that can be delivered and a weaker penetration depth made the IJV system has a huge advantage when compared to DV system (Hazim, 2017). This is also support by the study from Xiufeng Yang, et al (2019). Their simulation result indicate that the supply air always spreads along the whole floor when IJV is operated in cooling or isothermal scenarios, while in heating situation the warm supply air will separates from the floor in a short distance after spreading on the surface of the floor. This is because of the thermal buoyancy effect which make hotter air tend to flow upward while cold air flow downward. Due to this condition the air dispersion area over the floor in heating situation become limited. From their simulation also found out that in order to increase the warm air dispersion area the warm air supply nozzle has to place at lower height. Although this method will lead to a higher temperature near the floor within the zone of warm jet flow, but the average temperature around the room will still maintain the same. Where this is way better than using MV in heating scenario where the indoor air temperature is lower in the occupied zone and is higher in the upper zone.

2.3.1 Formula related to thermal comfort and indoor air quality

The parameters stated below are used to investigate the thermal comfort and indoor air quality of a contaminated area.

Draught rate/ Draft (DR) which describes the discomfort of a person experiences due to unwanted cooling of the human body causes by the air movement and it is estimated by the following equation (Arman Ameen, et al, 2019; ISO 7730, ASHRAE 55-2004):

$$DR = (3.14 + 0.37 \cdot u_a \cdot I_p)(34 - T_a)(u_a - 0.05)^{0.62} \qquad (2.1)$$

$$For\ u_a < 0.05\frac{m}{s}\ use\ u_a = 0.05\frac{m}{s}; For\ DR > 100\%\ use\ DR = 100$$

Where u_a is the mean air velocity, m/s, I_p is the local turbulence intensity, % and T_a is the local temperature, °C. A high draught rate indicates that the air flow at the certain place will bring uncomfortable experience to the people who stay at the place.
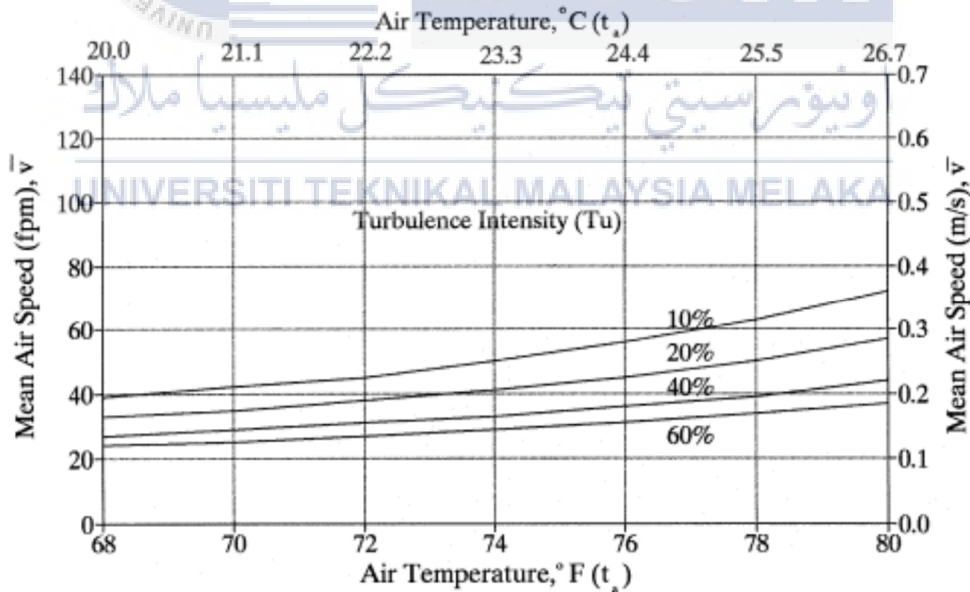
Figure 2.7: Allowable Mean Air Speed as a function of air temperature and turbulence intensity (ASHRAE 55-2004)

Percentage dissatisfied (PD) which is related to the local discomfort due to a high vertical air temperature difference between head and ankle and it is estimated by the following equation (Arman Ameen, et al, 2019; ISO 7730):

$$PD = \frac{100(\%)}{1 + exp(5.76 - 0.856 \cdot \Delta T_{0.1-1.1})}$$ (2.2)

Where $\Delta T_{0.1-1.1}$ is the temperature difference between ankle and neck level of seated people.

Temperature effectiveness (ε_T) is a parameter that can be used to evaluate the effectiveness of heat removal (Arman Ameen, et al, 2019; Nielsen, 1993),

$$\varepsilon_T = \frac{(T_o - T_i)}{(\bar{T}_{0.1,0.6,1.1} - T_i)}$$ (2.3)

Where $\bar{T}_{0.1,0.6,1.1}$ is the arithmetic mean air temperature of the heights 0.1, 0.6, and 1.1 m, °C, T_o is the outlet air temperature, °C and T_i is the supply air temperature, °C.

AEE, ε_a, air-exchange efficiency is defined as the ratio of the nominal turnover time to the average time of exchange of air in the room (CLIFFORD C. FEDERSPIEL, 1999).

$$\varepsilon_a = \frac{\tau_n}{2\alpha}$$ (2.4)

Where τ_n is the nominal turnover time which is defined as the ratio of the mass of air in the zone to the outdoor air mass flow rate, α is the volumetric mean age of the air.

ACE, ε_r, relative air change effectiveness is a ventilation performance measure referred to the system that do not recirculate air which is defined as the value of the air-exchange efficiency where the recirculation fraction as zero (Clifford c. federspiel, 1999).

$$\varepsilon_r = \frac{\tau_n - \alpha_s}{2(\alpha - \alpha_s)}$$ (2.5)

$$\alpha_s = \tau_n R$$ (2.6)

Where α_s is the age of the supply air, R is the fraction of return air that is recirculated to the supply. While the relationship of ε_a, ε_r and R is shown in Figure 2.8 below.

17
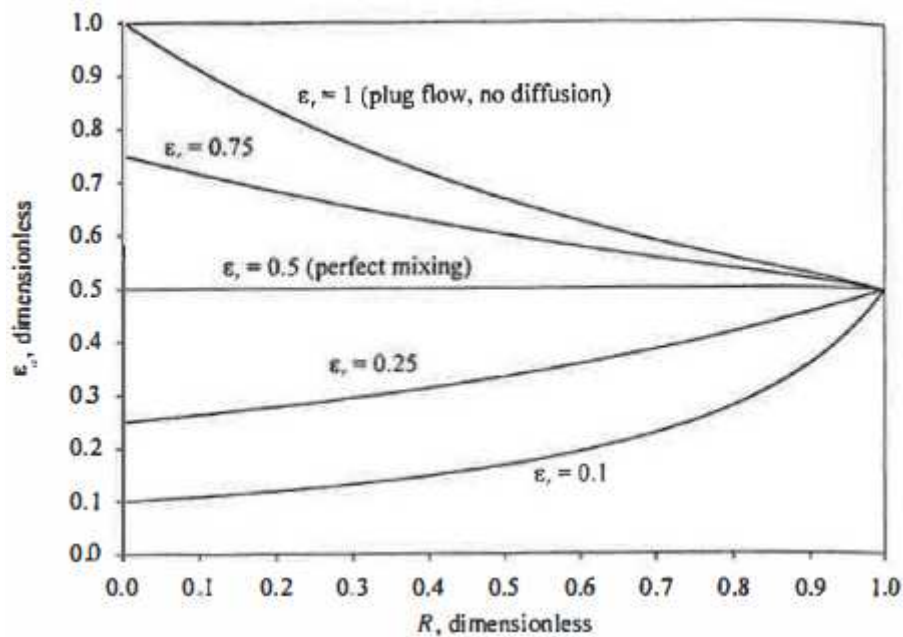
Figure 2.8: Relation between ε_a, ε_r and R (CLIFFORD C. FEDERSPIEL, 1999)

2.3.2 Effects of impinging jet ventilation system towards indoor air quality and thermal comfort

An experiment from Arman Ameen, et al (2019) have investigate about the behaviour of corner impinging jet ventilation system by comparing to traditional ventilation method which are mixing and displacement ventilation (Figure 2.9). The study found out that the corner impinging jet ventilation system (CIJV) is slightly better than DV system when considering the draught rate, this is due to the special design of the supply inlet for CIJV system. Besides that, CIJV also shows a high values of air change effectiveness and temperature effectiveness which means that CIJV can hit the required thermal comfort and IAQ at a lower energy usage. This study stated that typical DV systems are not designed for heating mode, which is believed to be a shortcoming of the system because of the dominance of thermal forces to momentum forces while the impinging jet system with higher momentum force in supply air can overcomes this shortcoming.

18
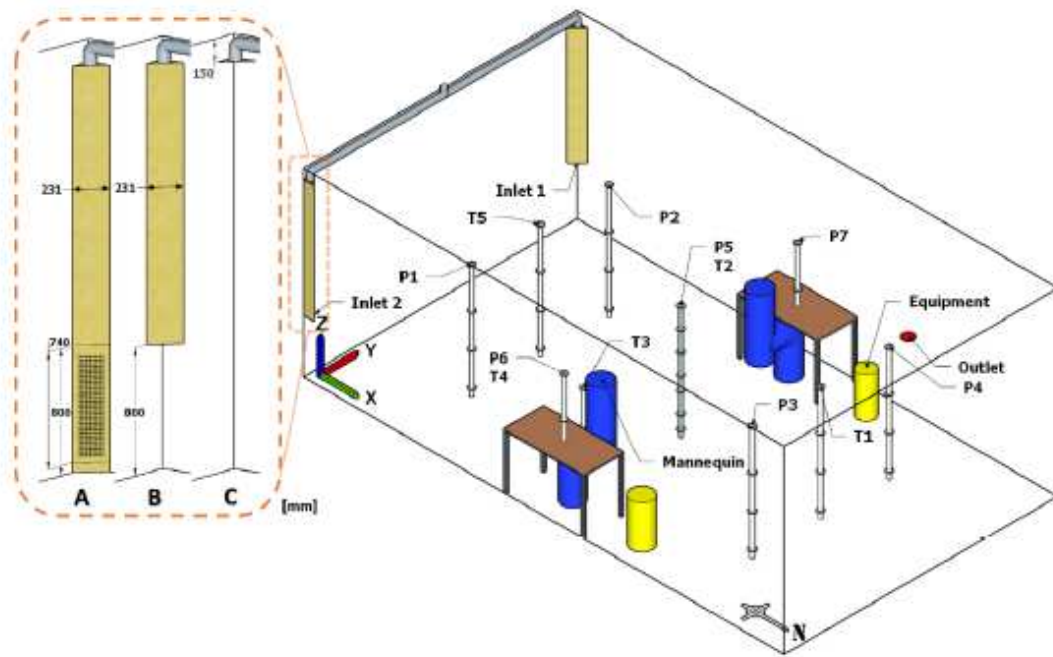
Figure 2.9: Layout Of The Test Chamber. A is displacement ventilation, B is corner

impinging jet ventilation, C is mixing ventilation (Arman Ameen, et al, 2019)

Besides that, by splitting the return vent from the exhaust device in the IJV system,

the energy efficiency of the whole system can be further improved. In the present study by

Ye, et al (2020), numerical simulations are performed to determine the relationship

between the thermal comfort indices (draught comfort (PD) and temperature gradient

between the head and ankle levels (ΔT)), IAQ indices (air change efficiency (ACE) and

contaminant removal efficiency (ε)) and energy efficiency index (η) for an IJV system with

return outlet height (H) ranged from the ceiling to the floor level. The results show that

when the H increases, the values of ΔT and η decrease, meanwhile the values of PD, ACE

and ε increase. At the end of the discussion in article, they presented a recommendation

graph which present the optimal range of H is 1.2–1.5 m above the floor to achieve the best

overall performance of IJV (Figure 2.10). Moreover, they also present a comprehensive

graph of H which could provide directions for optimizing the positions of exhaust and

return devices (Figure 2.11).

19
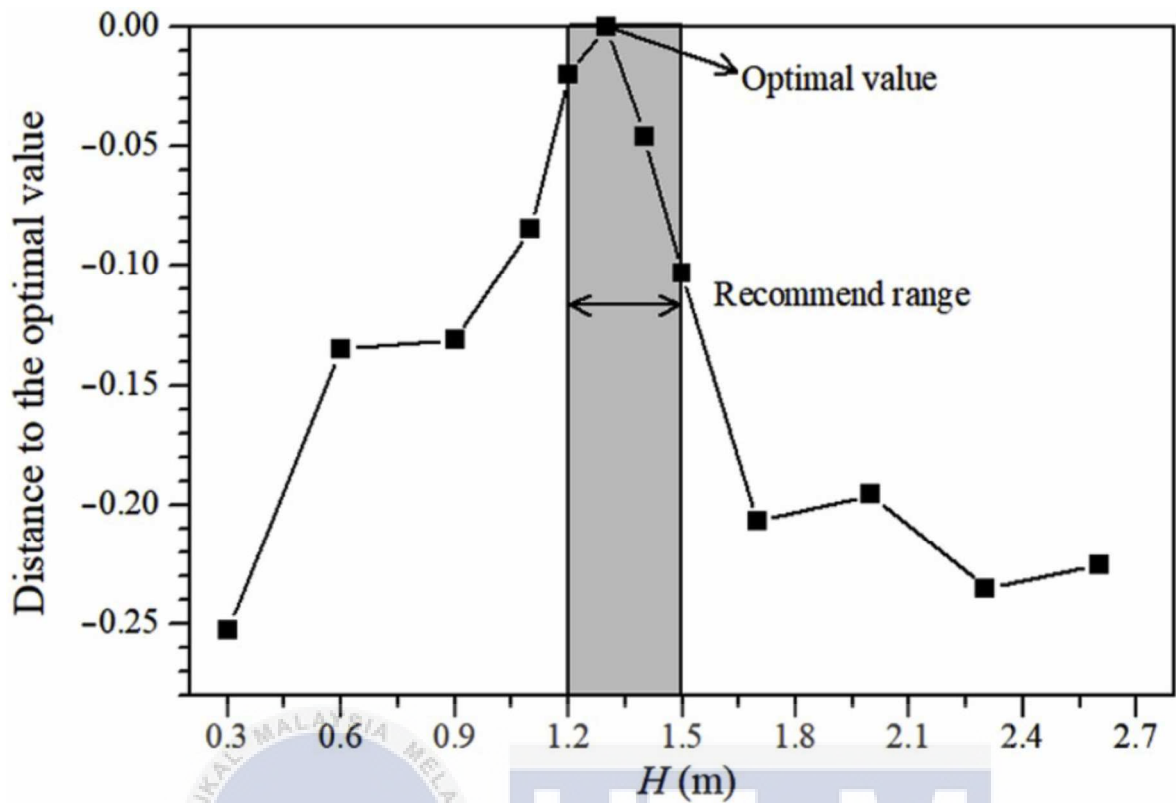
Figure 2.10: Distance between the recommended and optimal return vent height (Ye, et al, 2020)
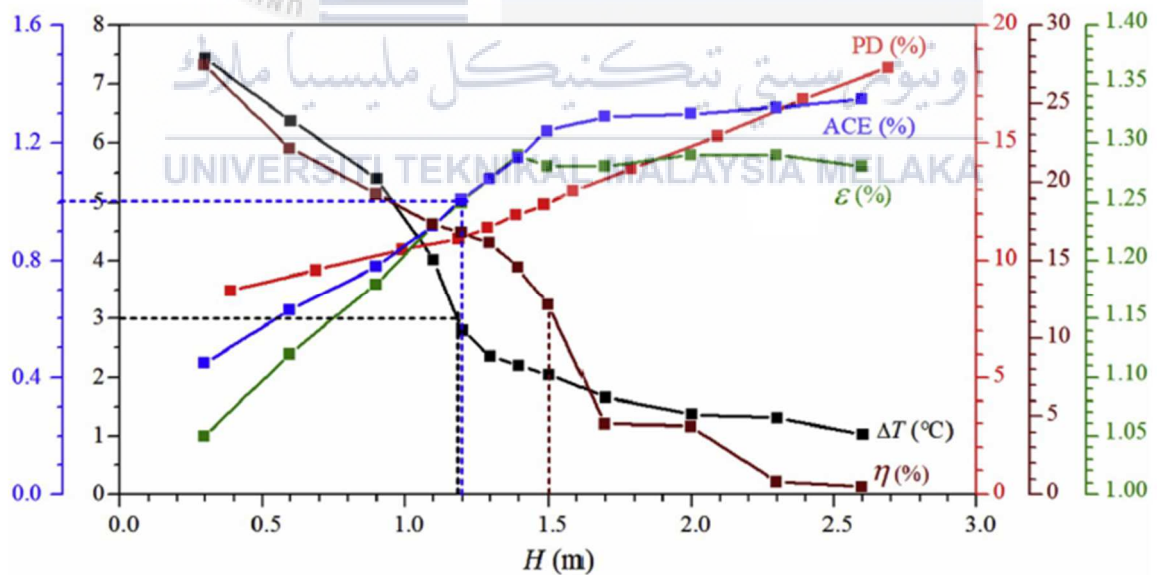
Figure 2.11: Comprehensive indices at different values of H (Ye, et al, 2020)

Next, a study by Samira Haghshenaskashani and Behrang Sajadi (2018) backs up the claim that the IJV system's energy efficiency can be increased by separating the return vent from the exhaust device. Their findings demonstrate that the location of the return air vent has a significant impact on the impinging jet ventilation system's thermal comfort and energy consumption, but only a little impact on the draught discomfort criteria. The lower the return air vent level, the worse the PMV thermal comfort index, according to the CFD simulation results. In addition, employing the ceiling exhaust minimises PMV. Furthermore, depending on the required inlet air temperature, ceiling exhaust can cut energy usage by up to 30% while also lowering the vertical temperature gradient in the space.

Predict Mean Vote (PMV) is an empirical index and it has been developed based physiologically on a steady-state model of thermal exchanges between the human body and the environment (Guodong Ye, et al, 2003).

$$PMV = [0.303\,exp(-0.036M) + 0.028] \times L \qquad (2.7)$$

$$
\begin{aligned}
L = (M - W) &- 3.96 \times 10 - 8\,f_{cl}[(t_{cl} + 273)4 - (t_r + 273)4] \\
&- f_{cl}h_c(t_{cl} - t_a) - 3.05[5.73 - 0.007(M - W) - p_a] \\
&- 0.42[(M - W) - 58.15] - 0.0173M(5.87 - p_a) \\
&- 0.0014M(34 - t_a) \qquad (2.8)
\end{aligned}
$$

Where L - thermal load on the body (W/m2);

M - metabolic rate of human body (W/m2);

W - rate of mechanical work accomplished (W/m2);

ta - air temperature;

tr - mean radiant temperature;

fcl - clothing area factor, dimensionless;

tcl - mean temperature of the outer surface of the clothed body;

hc - convective heat transfer coefficient (W/(m2·°C)).

pa - water vapor pressure in ambient air (kPa).

The result from the study done by Chao Qin, et al (2020) also shows that the location of ceiling exhaust will greatly affect the thermal comfort of the particular contaminated area. By bringing the ceiling exhaust closer to the source of the thermal plume, the heat created may be removed more efficiently. The researchers also discovered that placing the ceiling exhaust in the geometrical centre of a large space can result in a longer mean age of air (MAA) than placing it on the sides. For the recirculation of impinged air, placing it on the same side as the air provider results in a more equal MAA distribution than placing it on the opposite side of the air source.

Local mean age of air is defined as the average time needed for air to reach a certain location since it entered the room. By solving an additional partial differential equation, the local mean age value θ can be calculated. The equation is derived from the concentration equation for numerical purposes, with the assumption that contamination generation is homogeneous across the room. The equation is shown in its final form below:

$$\frac{\partial}{\partial x}\left[\rho u\theta - \left(\frac{\mu}{\sigma_l} + \frac{\mu_t}{\sigma_t}\right)\frac{\partial\theta}{\partial x}\right] + \frac{\partial}{\partial y}\left[\rho v\theta - \left(\frac{\mu}{\sigma_l} + \frac{\mu_t}{\sigma_t}\right)\frac{\partial\theta}{\partial y}\right] + \frac{\partial}{\partial z}\left[\rho w\theta - \left(\frac{\mu}{\sigma_l} + \frac{\mu_t}{\sigma_t}\right)\frac{\partial\theta}{\partial z}\right] = 1 \qquad (2.9)$$

where u, v and w are the velocity components, ρ is the density of air, μ and μt are the physical and turbulent viscosities, σ_l and σ_t are the laminar and turbulent Schmidt numbers (Bartak M, et al, 2001).

Ala'a Abbas Mahdi and Sara Mohammed Abbas (2018) had carried out an experiment to investigate about the effects of different cross sectional area of supply duct towards impinging jet ventilation. From the experiment they found out that the square shape air supply duct can provide a comfort environment comparing to the semi-elliptic shape duct and rectangle shape duct. Moreover, the square shape supply duct was found that the ventilation efficiency, effective temperature and also optimum air distribution performance index (ADPI) in terms of human thermal comfort and indoor air quality

perform better compare to other types of duct. On the total number of points tested, the air distribution performance index (ADPI) is the percentage calculated by the number of measured points in an inhabited space where it is within the required limit (> -1.7 °C and 1.1 ° C). A literature index of 60 to 69 is inadequate, 70 to 79 is acceptable, and 80 and higher is considered a decent air distribution.

2.4   Summary

From all the review above had found out that the jet to plate distance (H/d ratio), design of the output nozzle and present of the exhaust and return duct plays an important row in affecting the efficiency of the impinging jet ventilation system toward the thermal comfort and indoor air quality. Hence in this project our aim to analyse the relationship of impinging jet ventilation with the position of exhaust, various nozzle shape and height of the closed area and propose a most efficient model is a meaningful and beneficial objective.
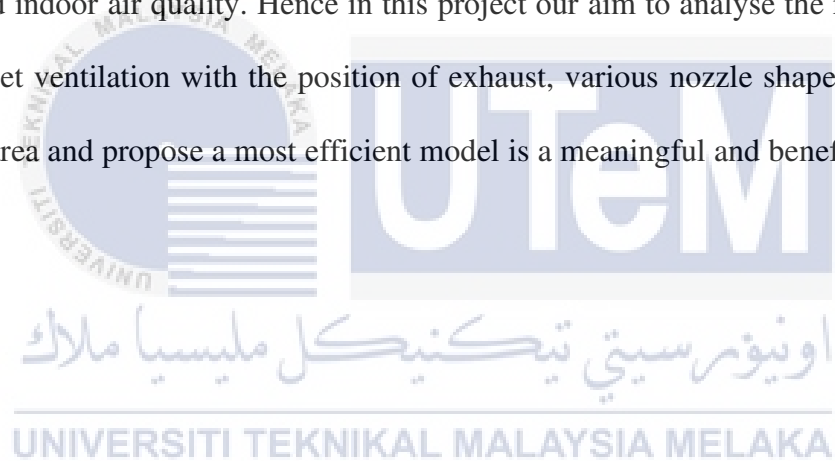
CHAPTER 3

METHODOLOGY

3.1   Overview

This chapter will discuss about the method and software used to carry out the analysis of the study for the impinging jet ventilation. The flowchart of the process to carry out this study is as follow.
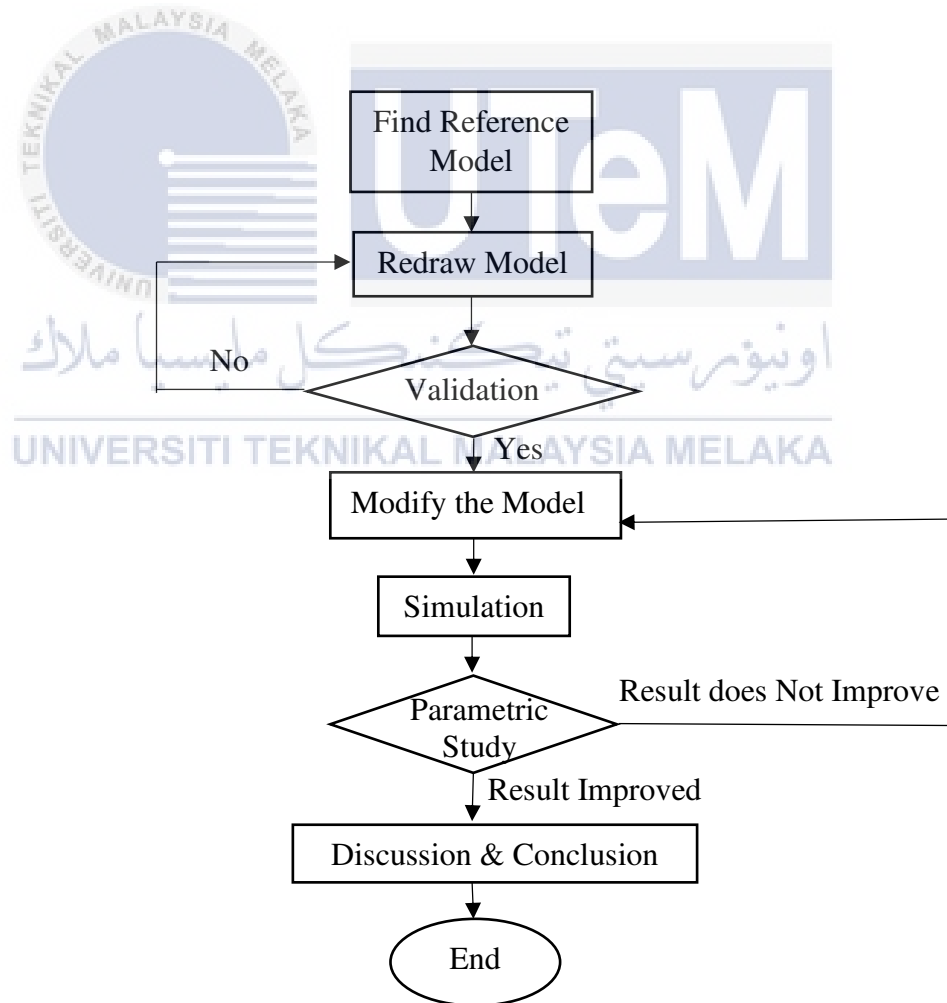
Figure 3.1: Flow Chart of Methodology

3.2   Model

3.2.1   Study cases

The reference model for this project is based on a laboratory office (Figure 3.2), of which thermal boundary properties were thoroughly published by Kobayashi, Sugita, Umemiya, Kishimoto, & Sandberg (2017). The size of the model is 9m x 5m x 2.7m where the inlet nozzle of the IJV system is install at the middle of the wall which having 5 meter long. The distance from the floor to the inlet nozzle of IJV system is 0.6m and the exhaust is located at the ceiling. A square shape box with 0.8m x 0.8m x 0.8m dimension is located at the middle of the room to act as a heat generator. The detail design of the laboratory is presented in the Figure 3.2 where the unit shown in the Figure is in meter.
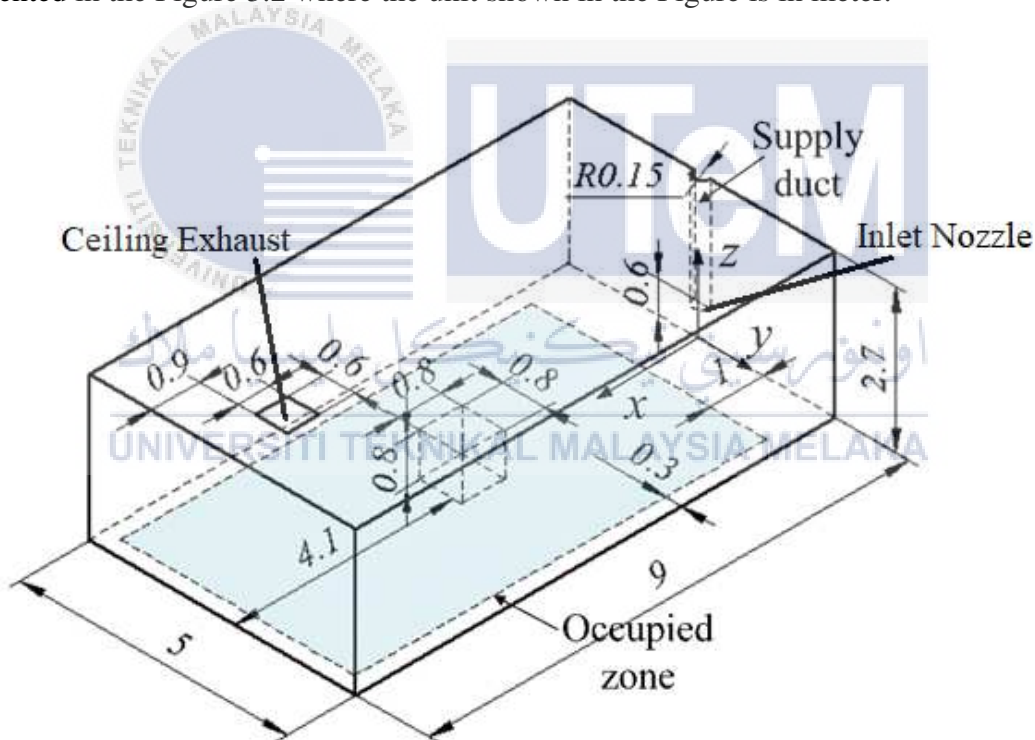
Figure 3.2: Full Scale Design of the Laboratory Office (Kobayashi, et al, 2017)

The manipulated variables for this study are the location of ceiling exhaust and the shape of the inlet nozzle for the impinging jet ventilation duct. Figure 3.2 is the drawing for first case out of 9 where the location of the ceiling exhaust is at downwind while the shape of the inlet nozzle is semicircle. Figure 3.3 shows all 3 location of ceiling exhaust

which are 'Downwind', 'Middle' and 'Upwind'. The 'Downwind' and 'Upwind' means the downwind and upwind of heating source and 'Middle' is at middle of the laboratory office. The 'Downwind' ceiling exhaust located at 7.5m away from the wall equip with the impinging jet inlet nozzle while the 'Middle' ceiling exhaust is 4.2m away and the 'Upwind' ceiling exhaust is 0.9m away.
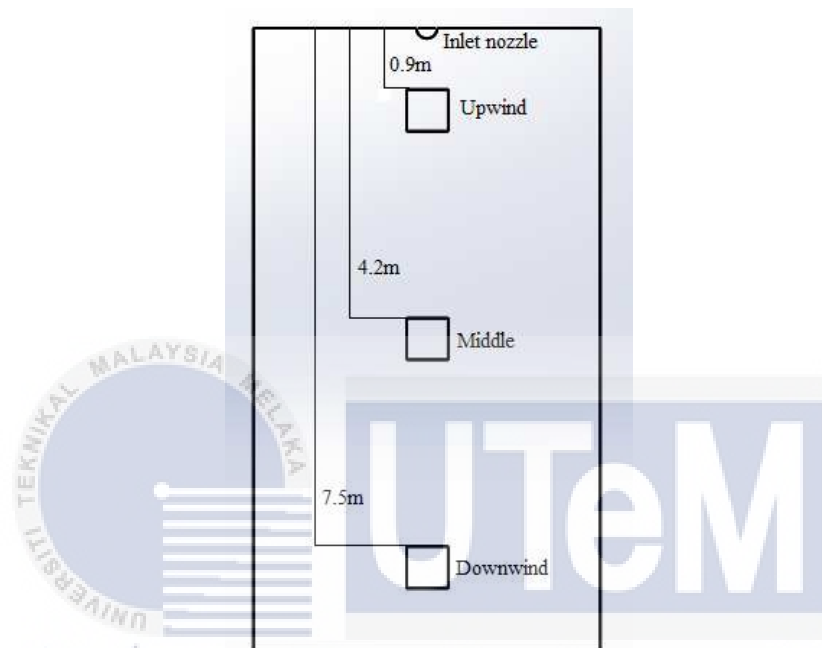
Figure 3.3: Location of Ceiling Exhaust
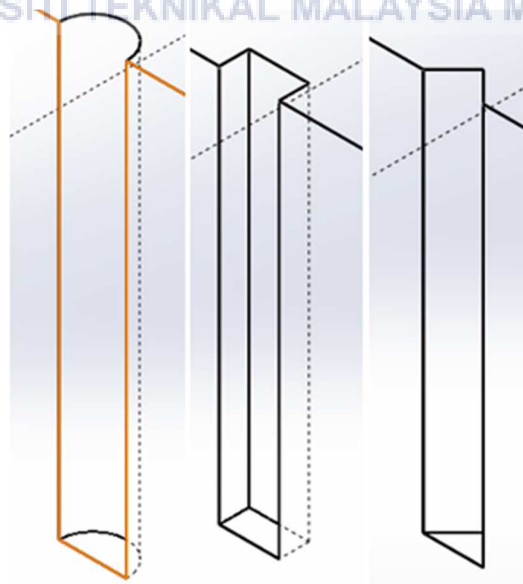
Figure 3.4: Type of Inlet (semicircle, rectangle, triangle)

Figure 3.4 shows all 3 types of nozzle which are semicircle shape, rectangle shape and triangle shape. The specification of each model in listed in the Table 3.1.

Table 3.1: Specification of the investigate models

Case No.	Location of ceiling exhaust	Shape of the inlet nozzle
1	Downwind	Semicircle
2	Downwind	Rectangle
3	Downwind	Triangle
4	Middle	Semicircle
5	Middle	Rectangle
6	Middle	Triangle
7	Upwind	Semicircle
8	Upwind	Rectangle
9	Upwind	Triangle

In all cases, the occupied zone (the light blue zone in Figure 3.2) is 1.8 m above the floor, 1 m away from the discharge wall and 0.3 m from other walls according to the standard (ASHRAE, 2010). The heating source at the centre of the model is used to heat the surrounding air and create thermal plumes in order to test the ventilation performances of each case. The case study is carries out by comparing the effects of the exhaust location and the shape of inlet nozzle toward the air flow properties inside the room.

3.2.2 Numerical Models

3.2.2.1 Governing Equations

The mass and heat transfer in the model room is governed by mass, momentum and energy conservation laws (Navier-Stokes equations). Navier-Stokes equations is a partial differential equation that describes the flow of an incompressible fluid. While in steady state, the equations are:

$$\frac{\partial \rho u_i}{\partial x_i} = 0 \tag{3.1}$$

$$\frac{\partial \rho u_i u_j}{\partial x_j} = -\frac{\partial \rho}{\partial x_i} + \frac{\partial}{\partial x_j}\left(\mu \frac{\partial u_i}{\partial x_j}\right) + S_{Mi} \tag{3.2}$$

$$\frac{\partial(\rho C_v u_i T)}{\partial x_i} = p \frac{\partial u_i}{\partial x_i} + \frac{\partial}{\partial x_i}\left(\frac{\partial T}{\partial x_i}\right) + S_i \tag{3.3}$$

Where ρ is the air density, kg/m^3, u_i and u_j are the i_{th} and j_{th} component of velocity, ms^{-1}, i or j = 1, 2, 3 in a 3d space, S_{Mi} is the momentum sources, S_i is the sources of internal energy (including the changes in potential energy, but the heat generated by viscosity is neglected).

The ideal gas law is used to model thermal buoyancy effects where the gas flow is assumed to be incompressible while the volume of the gas flow is increase as the temperature of the gas increase. The including of this effects is aim to simulate the thermal plume in our simulation. Hence the density of the gas only varies with temperature and the formula is as shown in below:

$$\rho = \frac{P_{op}}{\frac{RT}{M_w}} \tag{3.4}$$

Where R is the universal gas constant (8.314 JK^{-1}mol^{-1}); M_w, the molecular weight of gas, 28.966 gmol^{-1}; P_{op}, operating pressure (1 atm).

3.2.2.2 Turbulent Model

The flow in this work is turbulent. Reynolds number is defined as:

$$Re = \frac{UL}{v} \tag{3.5}$$

Where U is the characteristic velocity, where in this case is the inlet velocity is calculated from flow rate 600m³/h which varies for different shape of inlet. For the cases with semicircle inlet the inlet velocity is 4.716 m/s, the L is the characteristic length (hydraulic diameter of supply duct, 0.367 m); v is the kinematic viscosity of air (1.79✕10-5 m²s⁻¹). As Re=116918 (> 2300), the flow is turbulent.

The Shear-Stress Transport (SST) k-w model is a two-equation eddy-viscosity model which can used to model the turbulent flow. The SST k-w model was formulated by F.R. Menter based on the SKE and k-w model proposed by Wilcox. This model included two different unique solutions to solve for two different condition in the problem which are k-w turbulence model is to compute the inner region of boundary layer and k-ε turbulence model is to compute the free shear flow away from the boundary. Because the SST k-w model accounts for the effect of turbulent shear stress transmission, it can be employed in turbulent flow fields with low Reynolds numbers without modifying the basic equation. In general, this model performs better in the impinging zone than the k- ε model because it includes an adjustment for the overestimation of k in the region. According to a previous research by Kobayashi, Sugita, Umemiya, Kishimoto, and Sandberg (2017), the SST k-w models' simulated findings were quite close to the observations. Turbulence kinetic energy equation and specific dissipation rate equation are two additional governing equations in the SST k-w model. The kinetic energy equation for turbulence is:

$$\rho \frac{\partial k u_i}{\partial x_i} = \frac{\partial}{\partial x_j}\left[\left(\mu + \frac{\mu_t}{\sigma_k}\right)\frac{\partial k}{\partial x_j}\right] + G_k - Y_k + S_k \tag{3.6}$$

The specific dissipation rate equation is:

$$\rho \frac{\partial \omega u_j}{\partial x_j} = \frac{\partial}{\partial x_j}\left[\left(\mu + \frac{\mu_t}{\sigma_\omega}\right)\frac{\partial \omega}{\partial x_j}\right] + G_\omega - Y_\omega + S_\omega \qquad (3.7)$$

3.2.2.3 The radiative heat transfer

The discrete ordinates (DO) model simulates radiative heat transfer to provide the local radiation temperature, which is an important parameter that influences the local temperature contour. In each octant of 4π solid angles of a point, this model solves the radiative heat transfer equation in $N\theta \times N\varphi$ directions. The air absorption and scattering effect are ignored in this study.

3.2.2.4 Boundary Conditions

The boundary conditions set in this study are follow by the reference article by Kobayashi, Sugita, Umemiya, Kishimoto, & Sandberg (2017). The inlet nozzle is set as velocity-inlet in the setup where the turbulence intensity for the air supply is set as 10% and turbulent length scale is 0.021 m according to the reported data of the reference article. The emissivity of each surface is: Ceiling and Floor, 0.85; Room wall, 0.1 (Aluminum-metalized) for the all the cases in this work including model validation case; Heating box, 0.02 (Polished). From the data in the reference article, they found out that in order to provide enough cold air for the large room (9 meters long), the supply air flowrate inside the article is 600 m³h⁻¹ hence the inlet velocity for semicircle inlet is 4.72 ms⁻¹. The detail for the boundary condition is presented in the Table 3.2.

Table 3.2: Boundary Conditions

Boundary	Thickness (mm)	External Temperature (^{o}C)	External convective conductance (Wm^{-2}K^{-2})	Thermal conductance (Wm^{-2}K^{-1})	Flowrate (m^3/h)
Floor	30	25.5	4.5	6	No slip
Ceiling	10	30	4.5	5.8	No slip
Wall	24	37	4.5	0.42	No slip
Heating	Heat flux 625 Wm^{-2}				No slip
Inlet	Temperature 19.27^{o}C; MAA 0s				600
Outlet	MAA: zero streamwise gradient				Outflow
Symmetry	-	-	-	-	Symmetry

The solver used in this study is ANSYS Fluent 19.2. The Pressure-velocity fields are coupled by the SIMPLEC (SIMPLE-Consistent). Gradient is discretized by the Least Squares Cell Based method, Pressure, the Body Force Weighted method and the convection terms, are the QUICK scheme. The gravitational force is set at -9.81 ms^{-2} in Y direction.

3.3   Model Validation

The model validation is based on the data from the article published by Kobayashi et al which is the selected reference article for this PSM. According to the article, the author had carried out their study by performing a full-scale laboratory experiment to obtained the real life data about a room ventilated by an impinging jet ventilation system. Next their study is continued by doing the CFD simulation of the impinging jet ventilation system of the full-scale laboratory experiment to compare the data obtained from the simulation and also the measured data from experiment. In their study, the flow and heat transfer inside the room was turbulent and the thermal buoyancy effect of the working fluid were included. This situation was similar to the process in our study, of which the thermal buoyancy effects is an important factor. Furthermore, their obtained data is presented clearly by using graph which can be easily compared the data obtain from this study.
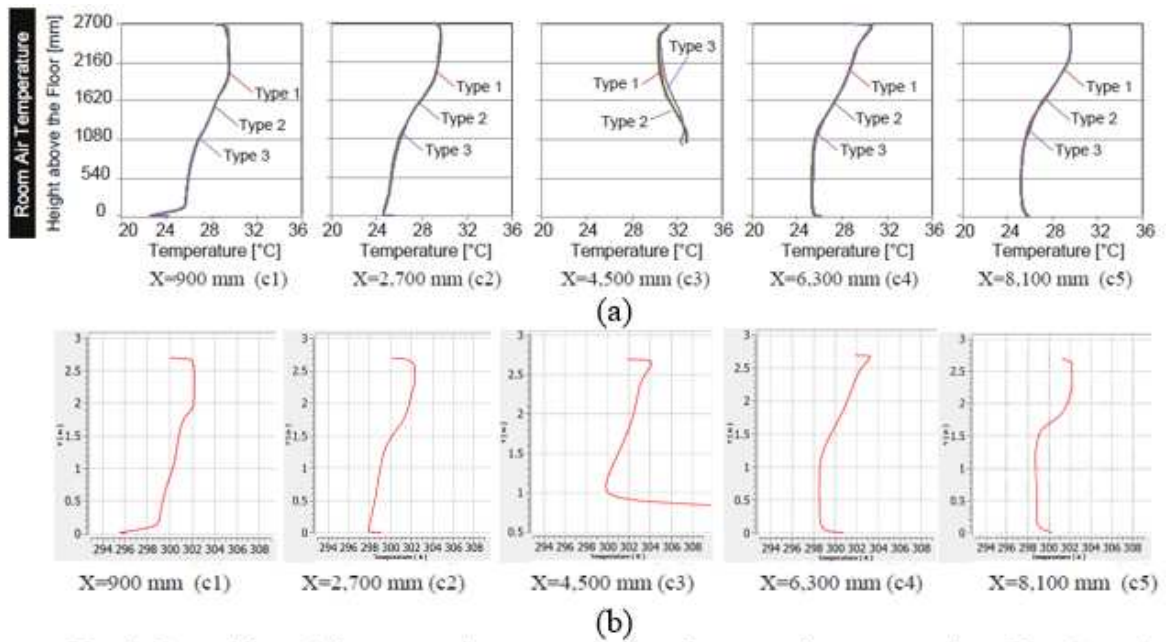
Vertical profiles of the room air temperature at the central cross-section (Y = 0 mm)

Figure 3.5: (a) Room Air Temperature graph from previous study (Kobayashi, et al, 2017)

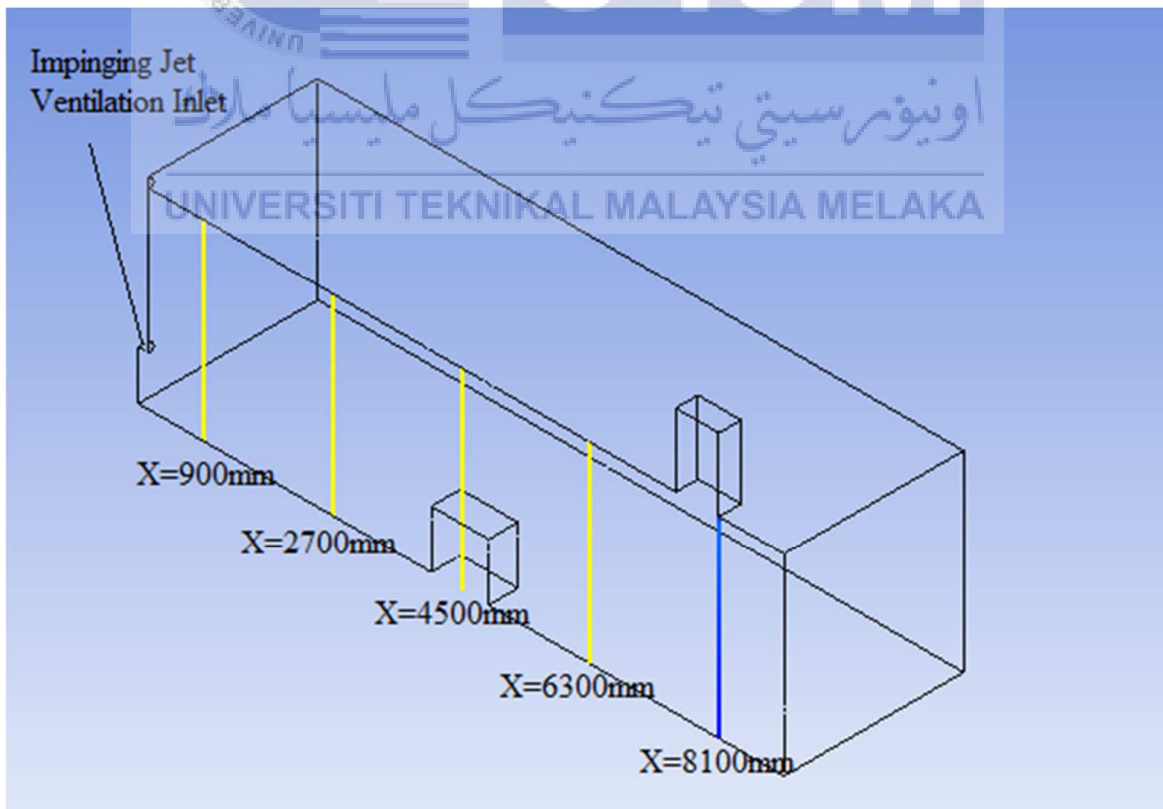(b) Room Air Temperature Graph from present CFD simulation

Figure 3.6: Location of data collected for the room temperature graph

The graph of height above the floor against the room air temperature from the article by Kobayashi, et al and from current CFD simulation is presented (Figure 3.5a and Figure 3.6a). The data source for the room temperature graph from CFD simulation is follow by the lines shown in the Figure 3.6 where position of the inlet of the impinging jet ventilation is count as 0 from X-axis, hence the room temperature graph at X=900mm is based on the line closest to the impinging jet ventilation inlet. The shape of the room temperature graph from CFD simulation and reference article match very well at X= 900mm and also X=2700mm where the graph at X=4500mm, 6300mm and 8100mm show discrepancies as the height closer to the ceiling. The possible reasons for discrepancies of the room temperature graph may due to the difference in meshing where the method of how to achieve the mesh they using did not clearly stated in the article.
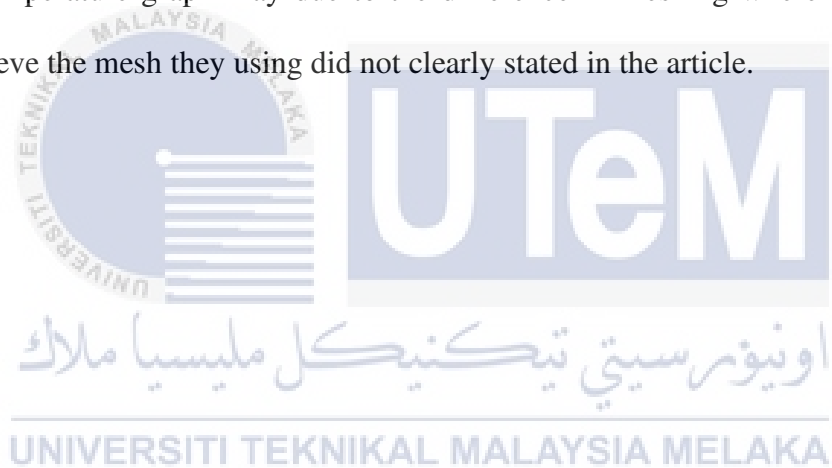
CHAPTER 4

RESULT AND DISCUSSION

4.1   Velocity field and flow pattern

In this section the air spreading distance along the floor after the air jet introduce to the room for each case are shown and the velocity profiles near the symmetry plane and vertical level from feet to head (sedentary and standing) for each case are presented. The velocity profile for the spreading distance is simulated from a plane which is 0.01m above the floor level, this is because the height of plane which lower than this value shows a zero air velocity along the plane in the simulation.

4.1.1   Air spreading velocity profile at plane near to the floor

The air spreading velocity profile for cases that exhaust is placing at downwind side which are case 1,2 and 3 are shown in Figure 4.1. From the Figure shown it can be seen that the air jet introduced into the room in case 2 and case 3 can travel much further compare with case 1. Due to the difference in the inlet nozzle shape the value for inlet air velocity in each case is also different in order to make sure the inlet air flowrate for each case is same as the inlet air flowrate stated in boundary conditions (600m^3/h). Hence the inlet air velocity for semicircle shape inlet (case 1) is 4.716 m/s; rectangle shape inlet (case 2) is 3.703 m/s; triangle shape inlet (case 3) is 7.407 m/s. This condition greatly affects the initial air spreading distance when introduce into the room in each case which the area of red contour in Figure 4.1c (case 3) is the largest and follow by Figure 4.1b (case 2) and the smallest one is Figure 4.1a (case 1). Besides that, it can be notice that the air flow at the

zone after the heating box (box at the middle of the model) for case 1 can be say at insignificant while the air flow for case 2 and case 3 is still noticeable.

Next in Figure 4.1a, it can be notice that the air is equally spread through the floor from the inlet nozzle until it reaches the wall. As the air approaches to the wall, the air flow is deflected from axial direction into vertical direction and create a streamline that flow along the region near the wall. This is due to the incident air from a later time collide with the deflected air and this force the air to flow in the vertical direction. This condition is similar in the case 2 and case 3 which is shown in Figure 4.1b and 4.1c.
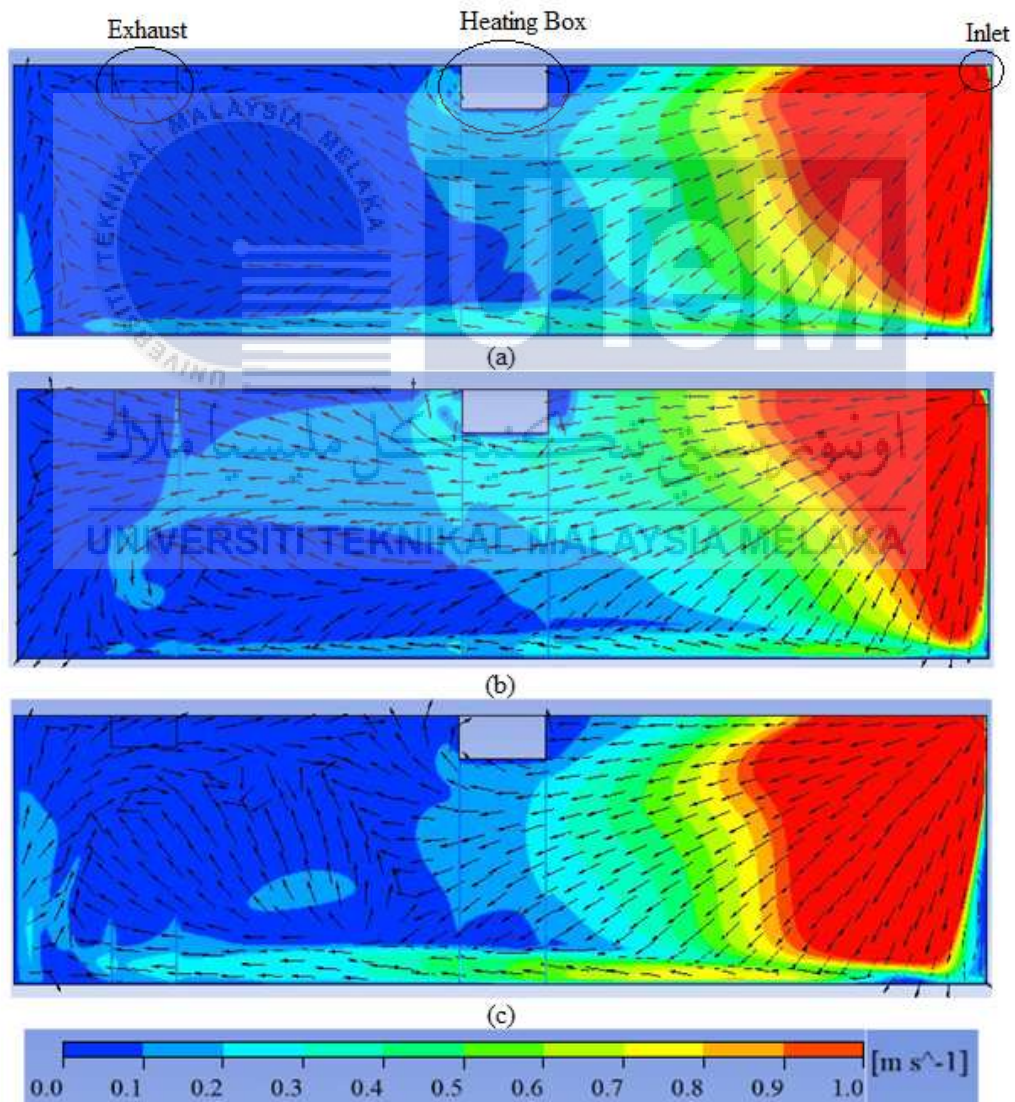

Figure 4.1: Velocity contour and Flow vector at plane 0.01m high from floor level (top view) for (a) Case 1, (b) Case 2, (c) Case 3

Meanwhile the simulated air flow pattern and velocity contour for all model in this project are presented in Figure 4.2 where Case 4 until Case 6 are the model exhaust is place at middle and Case 7 until Case 9 are the model exhaust is place at upwind. From the Figure 4.2, it can be notice that the result for Case 4 until 6 is similar with Case 1 until 3 where Case 1 is similar with case 4 and so on. Meanwhile the result for Case 7 and Case 9 shows a more vigorous air flow at the zone after the heating box compare to the cases with same shape of inlet nozzle in Case 1 until Case 6, while Case 8 is still the same with the other cases with shape inlet nozzle. Hence it can be conclude that as the position of exhaust more closer to the inlet nozzle of the IJV system the air spreading velocity profile along the floor will become more vigorous.
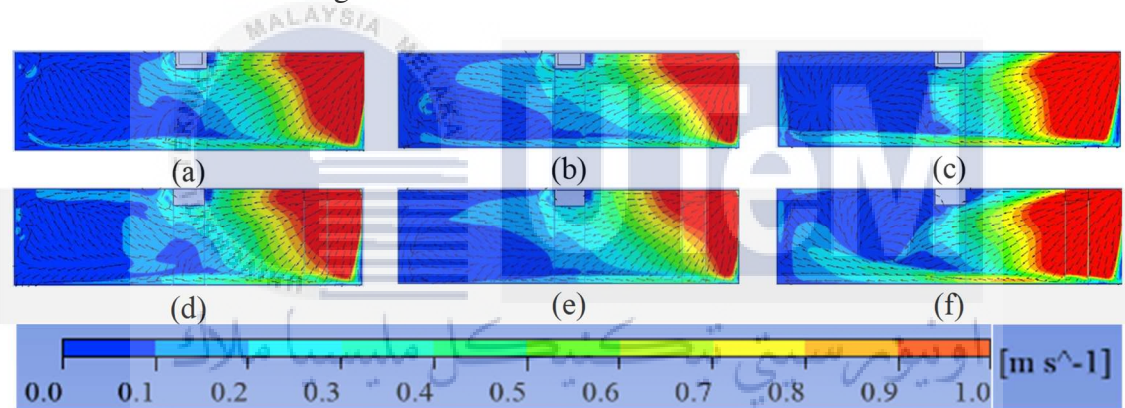

Figure 4.2: Velocity contour and Flow vector at plane 0.01m high from floor level (top view) for (a) Case 4, (b) Case 5, (c) Case 6, (d) Case 7, (e) Case 8, (f) Case 9

4.1.2   Flow field in the model

From the Figure 4.3a, it can be seen that the flow field on the symmetry plan for Case 1 can be separated into 3 zones which are the zone before heating box, the heating box zone and the zone after heating box. Each zone presents their own unique flow field. At the zone before heating box, the supply air from the inlet spread along the floor until the airflow reach the region after the heating box then flowing up to the exhaust on the ceiling. During the process of spreading, there are part of the air circulate up and flow back to the inlet when reaching the heating box region. This is due to the high velocity of the air at the inlet entrained the surrounding air to flow in the same direction and causing the air behind had to filling up the place that the surrounding air leaving. This situation forms air recirculate region which can be clearly seen at the zone before heating box in Figure 4.3a.

Next, the air flow in the heating box zone shows an upward airflow with velocity 0.4 m/s - 0.6 m/s. The upward airflow is due to the thermal plume create by the heating box. After the airflow reaching the ceiling, the airflow starts to spread through the ceiling while part of air spread to the downwind side is exiting the room through the exhaust. Meanwhile the other part of air spread to the upwind side of the room recirculate back to the heat plume and forming a whirlpool shape airflow which can be observe in Case 1 Z=2.5 m in Figure 4.4.

At the zone after the heating box, it can be told that all the air spreading from the inlet until this zone start to convert the flow direction from horizontal into vertical direction (Figure 4.3a). Besides that, from the Figure 4.3a it can be notice that the velocity of air flow at this zone is within 0 m/s to 0.2 m/s. Hence it can be said that the airflow in this region is mostly driven by the airflow created by the thermal plume and exhaust.

Figure 4.3: Velocity fields and streamlines on the symmetry plane (Side View) for (a) Case 1, (b) Case 2, (c) Case 3

From Figure 4.4, it can be seen that when z=2.5 m the flow field for Case 3 did not create a whirlpool at the upwind while Case 2 is on the edge of creation for the whirlpool airflow. Besides that, at standing (z=1.7 m) region the airflow in Case 3 is more vigorous compare to Case 1 and Case 2 where the air velocity contour for Case 3 shows a huge area of yellow (0.35 m/s) to light blue (0.1 m/s) contour at the upwind.

38

Figure 4.4: Velocity fields and streamlines (top view) for Case 1, Case 2 and Case 3 at vertical level from feet to head (sedentary and standing) and ceiling vicinity.

Figure 4.5 and Figure 4.6 shows the velocity profile for semicircle shape inlet with different exhaust location. It can be seen that the impact of exhaust location on the velocity field are limited near the floor and become more significant as approaching the ceiling level. Due to the exhaust location for Case 4 is at the top of the heating box, the airflow created by the thermal plume in this case direct flow to the exhaust and remove from the room instead of spreading along the ceiling like in Case 1 and Case 7 (Figure 4.5, Figure 4.6 z=2.5 m).

In terms of flow vectors the case with exhaust at upwind position (Case 7) presented a distorted flow at the zone before heating element compare to Case 1 and Case 5. This is due to both of the inlet and exhaust for Case 7 are located in the zone before the heating box which make the inflow and outflow of the air present in the same zone. Besides that, by placing the exhaust at middle and upwind location also affect the flow at the zone after the heating box. In Case 5 and Case 7 all the airflow at the zone after the heating box recirculate back to the heating box zone which can be seen in Figure 4.5.

While the velocity profile and flow field for rectangular shape inlet with different exhaust location (Figure 4.7, 4.8) is similar with the case with semicircle inlet (Figure 4.5, 4.6).

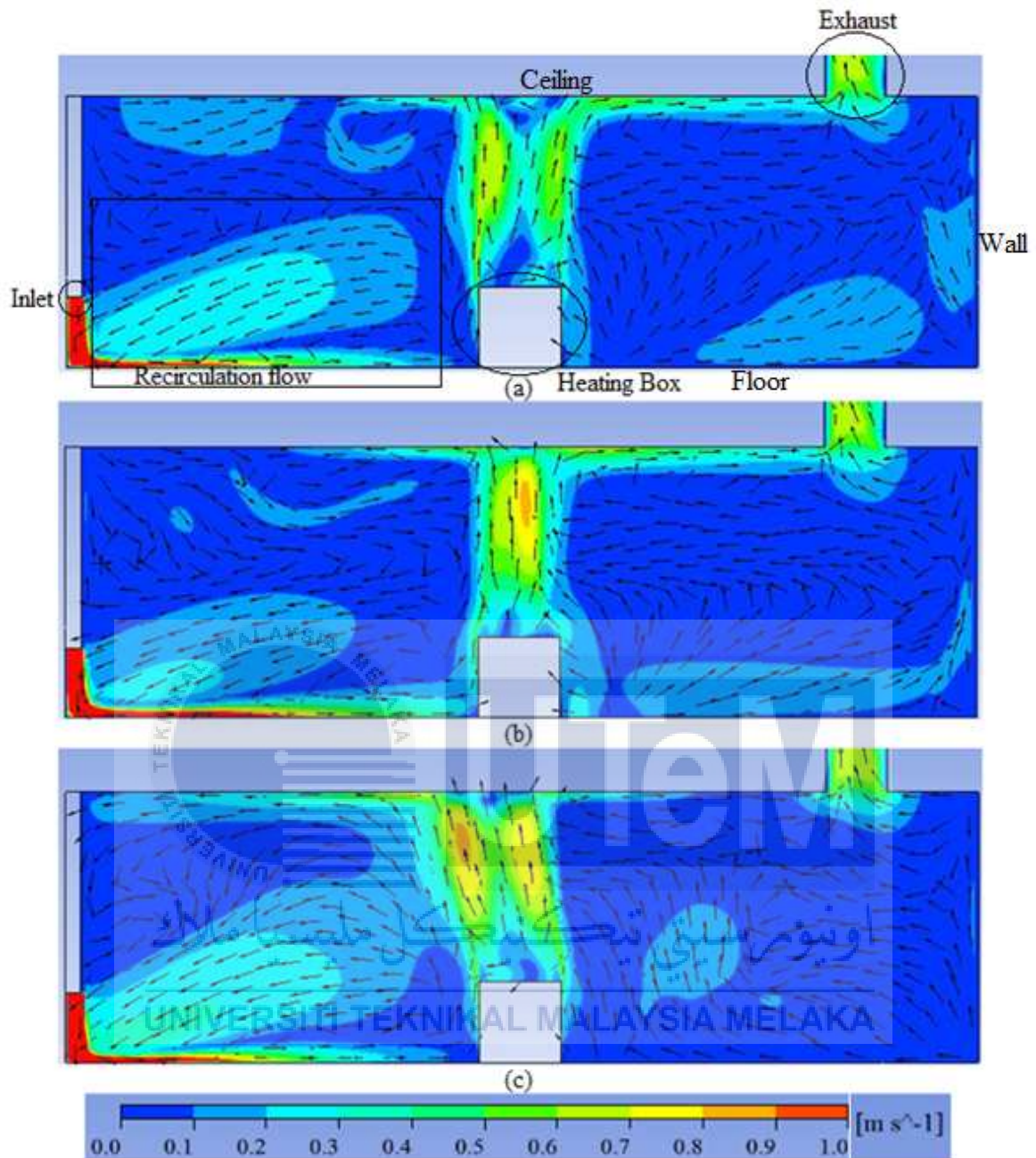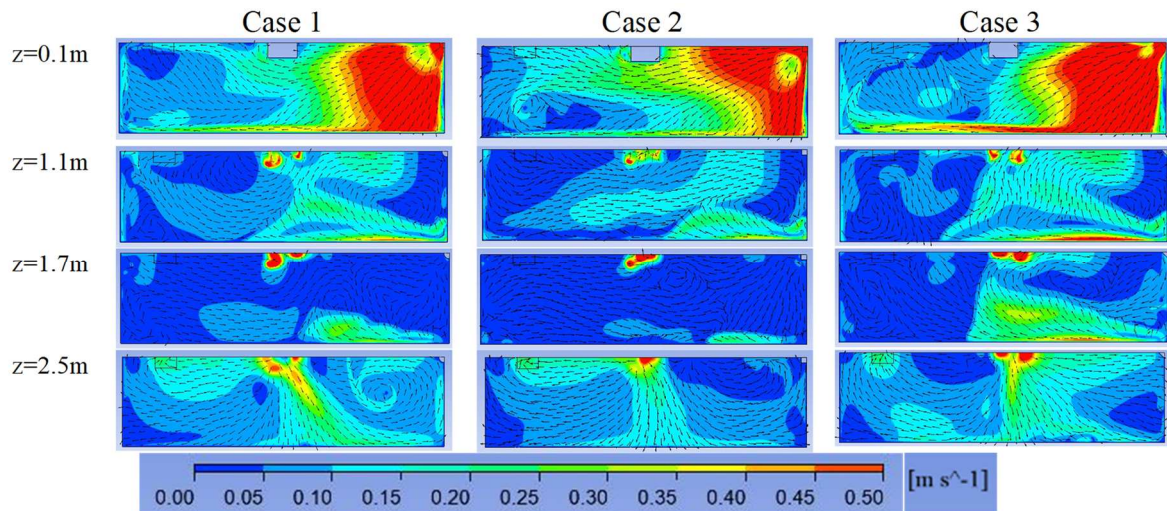
Figure 4.5: Velocity fields and streamlines on the symmetry plane (side view) for (a) Case 1, (b) Case 4, (c) Case 7

Figure 4.6: Velocity fields and streamlines (top view) for Case 1, Case 4 and Case 7 at vertical level from feet to head (sedentary and standing) and ceiling vicinity.
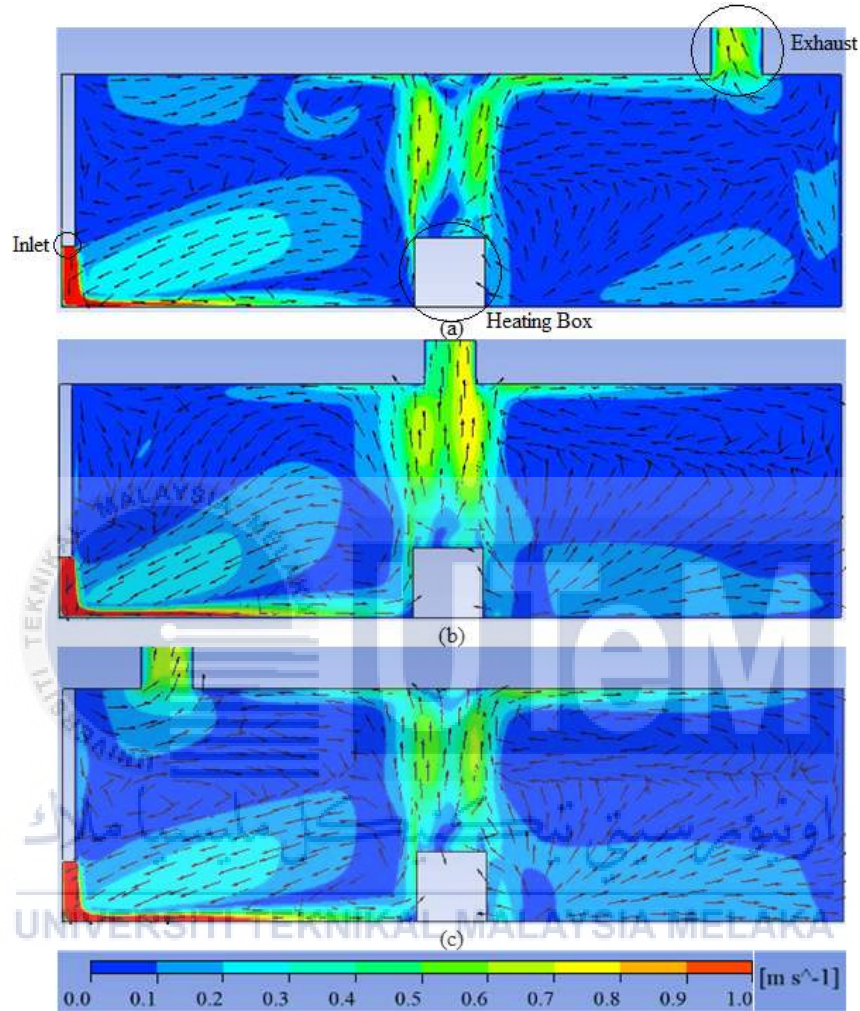

Figure 4.7: Velocity fields and streamlines on the symmetry plane (side view) for (a) Case 2, (b) Case 5, (c) Case 8
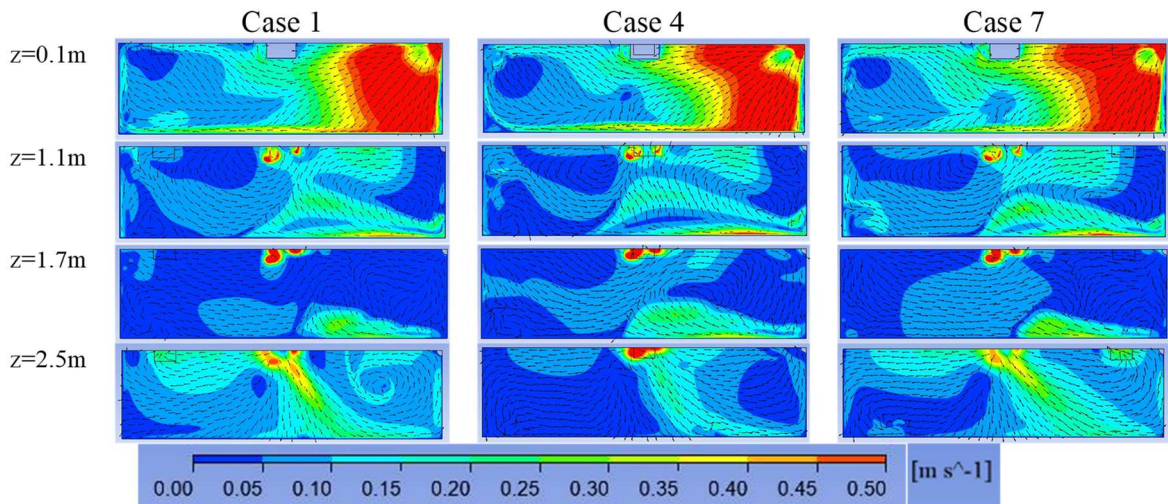
Figure 4.8: Velocity fields and streamlines (top view) for Case 2, Case 5 and Case 8 at vertical level from feet to head (sedentary and standing) and ceiling vicinity.
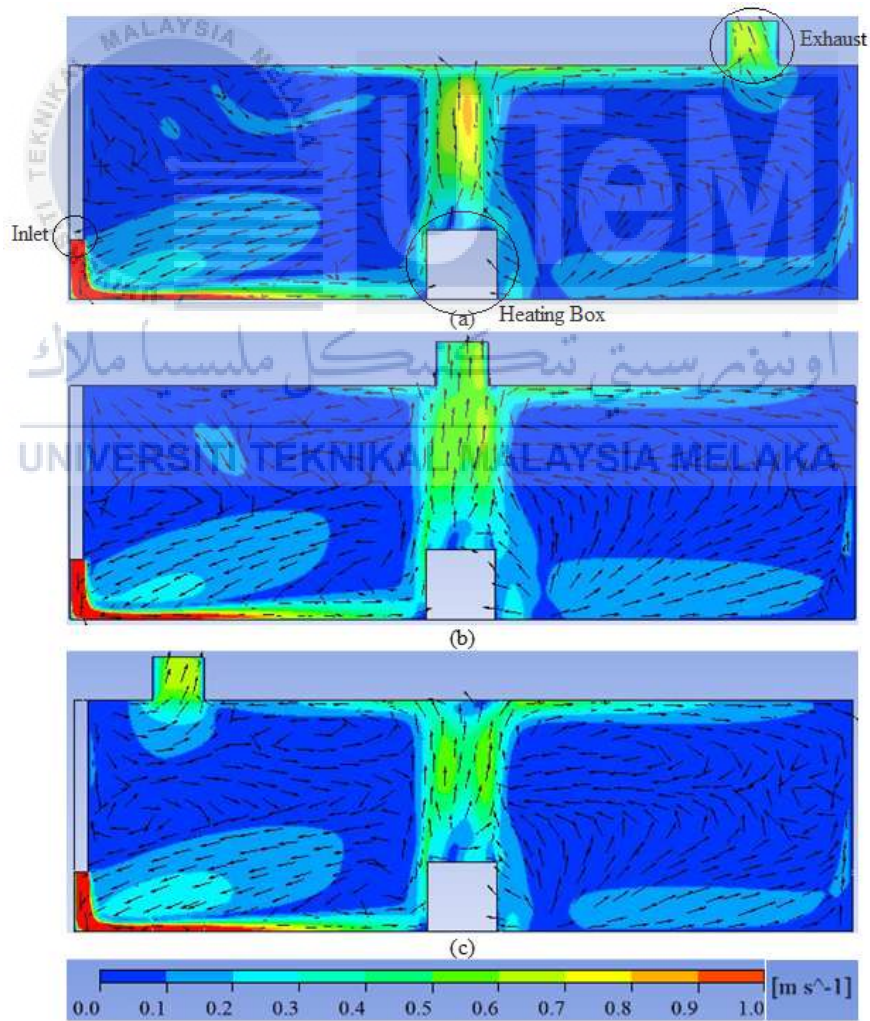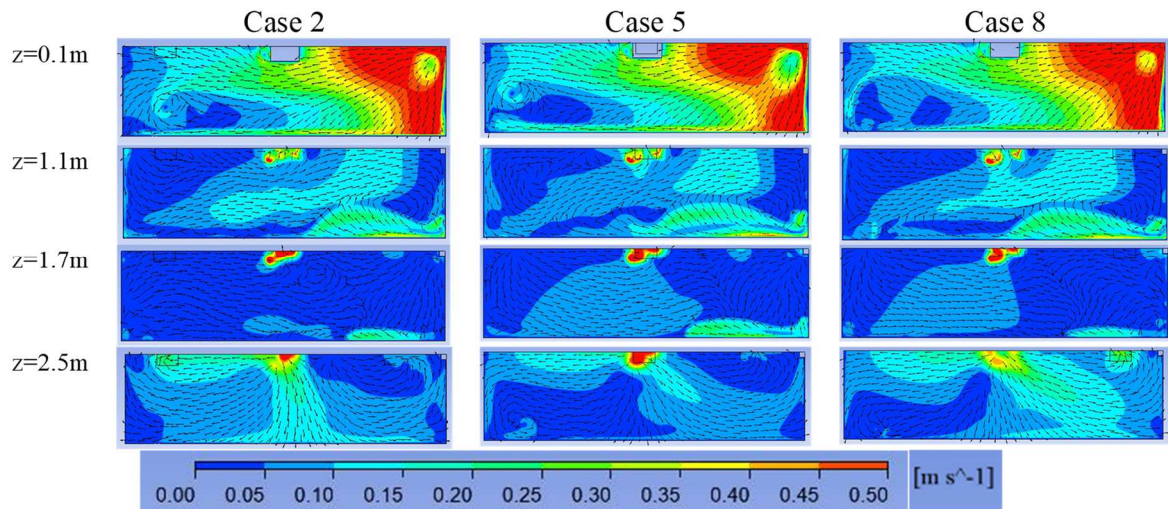
Although in the cases of using semicircle and rectangular shape inlet show a limited impact on the velocity field with various exhaust location at the region between standing (z=1.7m) and floor level (z=0.1m) but in the case with triangular inlet it shows a huge effect on it. From the Figure 4.9 and Figure 4.10, it can be seen that the velocity contour for the thermal plume on change as the location of exhaust change. In Case 6 the thermal plume created by the heating box directly flow into the exhaust above while for Case 9 the thermal plume is drag towards the exhaust by the recirculate flow causes by the inlet flow (which has been discuss at the beginning of this section) and also the outflow at the exhaust. This condition make the zone behind the heating box experience a relative low velocity airflow compare to the heating box zone in both Case 6 and Case 9. The average value of velocity for each plane in vertical level (z = 0.1 m, 1.1 m, 1.7 m, 2.5 m) are presented in Table 4.1 and it further clarify the discussion that had made before.
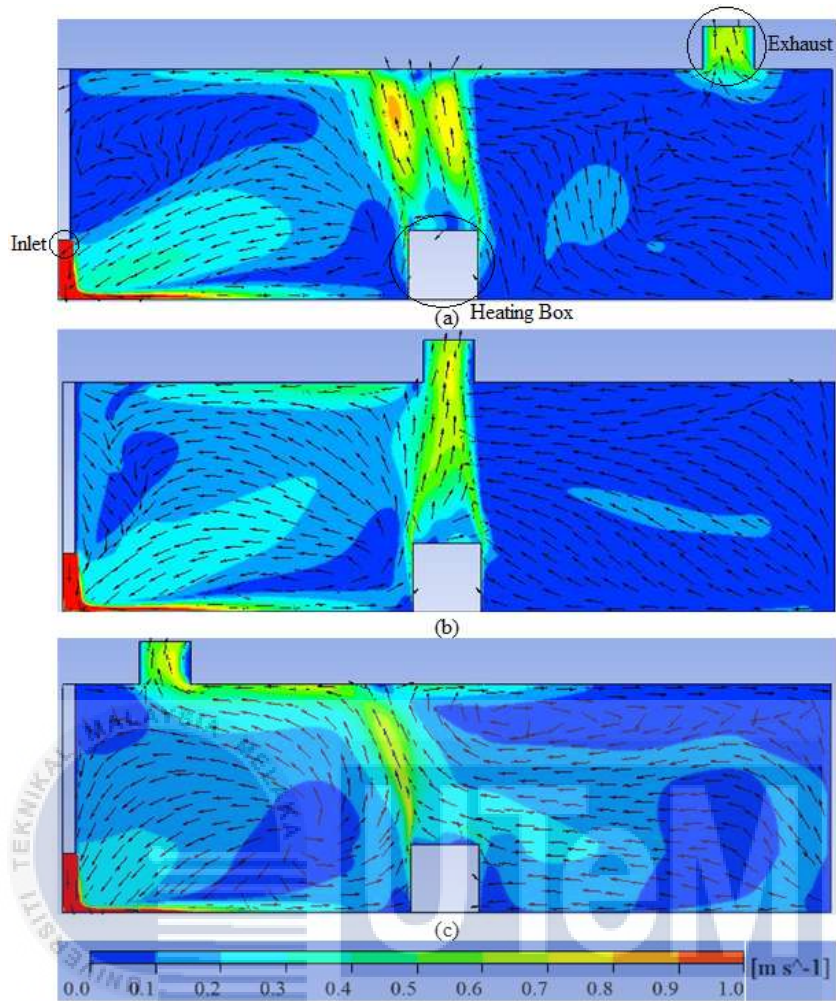
42

Figure 4.9: Velocity fields and streamlines on the symmetry plane (side view) for (a) Case 3, (b) Case 6, (c) Case 9
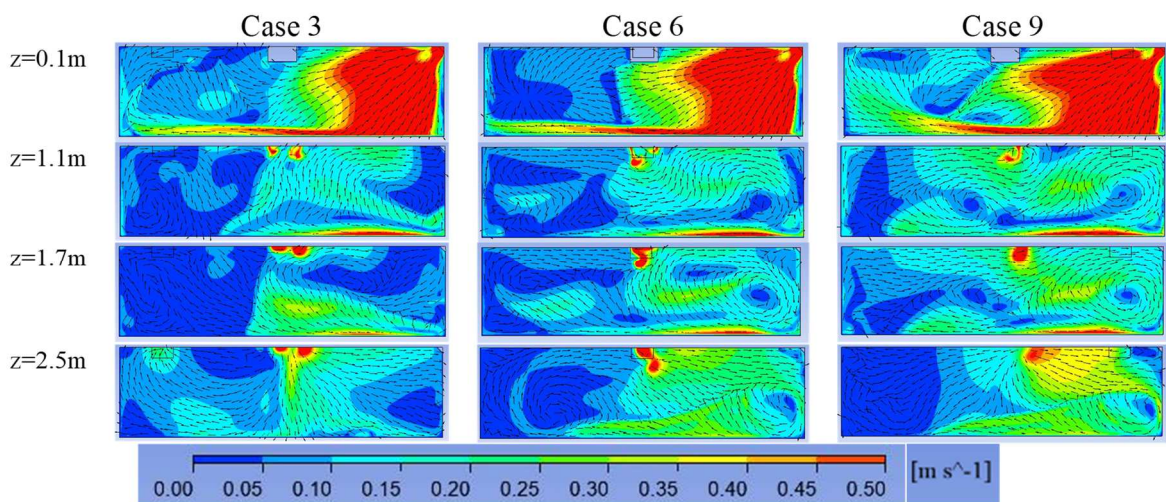

Figure 4.10: Velocity fields and streamlines (side view) for Case 3, Case 6 and Case 9 at vertical level from feet to head (sedentary and standing) and ceiling vicinity.

43

Table 4.1: Average velocity on each plane at vertical level from feet to head (sedentary and standing) and ceiling vicinity

	Velocity (m/s)			
Z (m)	0.1	1.1	1.7	2.5
Case 1	0.23387	0.09280	0.05611	0.10779
Case 2	0.22498	0.08608	0.04121	0.08378
Case 3	0.28296	0.10131	0.08751	0.10070
Case 4	0.24329	0.08621	0.07562	0.06099
Case 5	0.22443	0.08602	0.05935	0.06359
Case 6	0.29646	0.11568	0.11963	0.13676
Case 7	0.25013	0.10047	0.06397	0.10086
Case 8	0.23489	0.08864	0.04837	0.09292
Case 9	0.32762	0.14555	0.14710	0.14980

Based on the ICOP on IAQ 2010 which has been discuss in Section 2.1.2, the acceptable range for air movement in a building are within 0.15 m/s to 0.5 m/s. From the Table 4.1, it can be notice that from Case 1 to Case 9 except the plane $z = 0.1$ m all others plane shows an air velocity value lower than the acceptable range in ICOP where Case 9 is the closest case to the acceptable range. Hence in this section Case 9 shows its strength on air velocity compare to all other cases when the ICOP standard is take into account.

4.2 Temperature field and vertical temperature gradient

In this section the temperature distribution on the symmetry plane (Figure 4.11) and graph of vertical height Z, m against room air temperature, K for all cases on symmetry plane at X= 0.9 m, 2.7 m, 4.5 m, 6.3 m and 8.1 m (Figure 4.12) for each case are shown. From Figure 4.11 it can be seen that the temperature distribution along the symmetry plane for the cases with the exhaust insert at middle location are generally lower than other 6 cases with exhaust at upwind and downwind location. This is due to the thermal plume generate by the heating box are able to remove immediately when the exhaust is place above the heating box. Besides that, it can also notice that the temperature distribution for all the cases equip with triangular shape of inlet are more equally spread throughout the domain when comparing to other cases. Figure 4.12 provide a quantitative prove where Case 4, 5 and 6 are always lowest three cases when comparing to other cases.
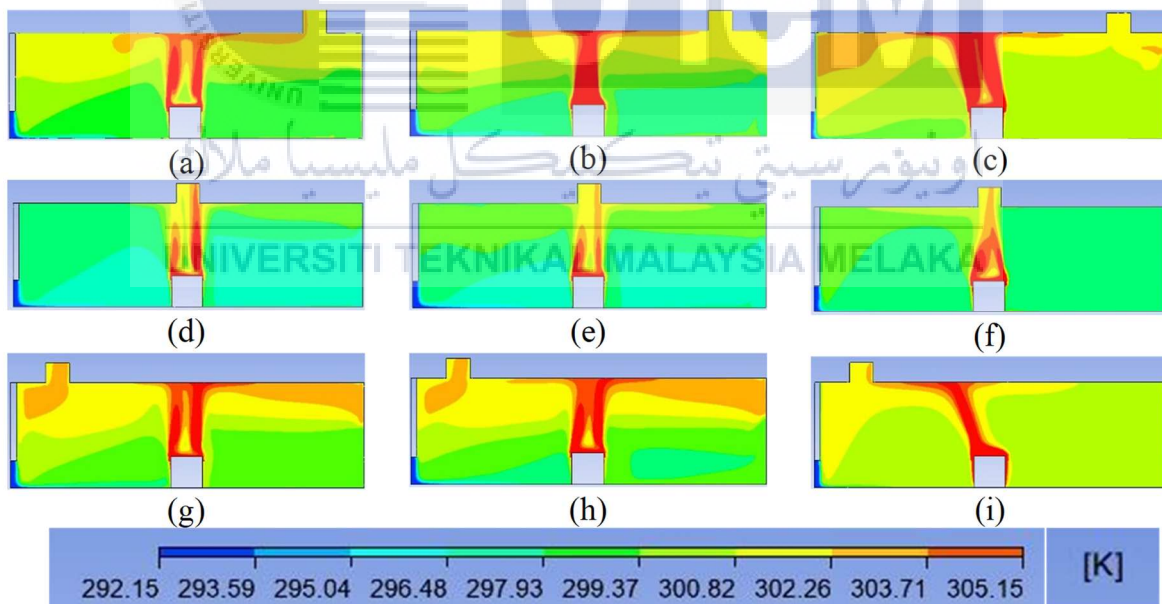
Figure 4.11: Temperature distribution on the symmetry plane (top view) (a) Case 1, (b) Case 2, (c) Case 3, (d) Case 4, (e) Case 5, (f) Case 6, (g) Case 7, (h) Case 8, (i) Case 9

45
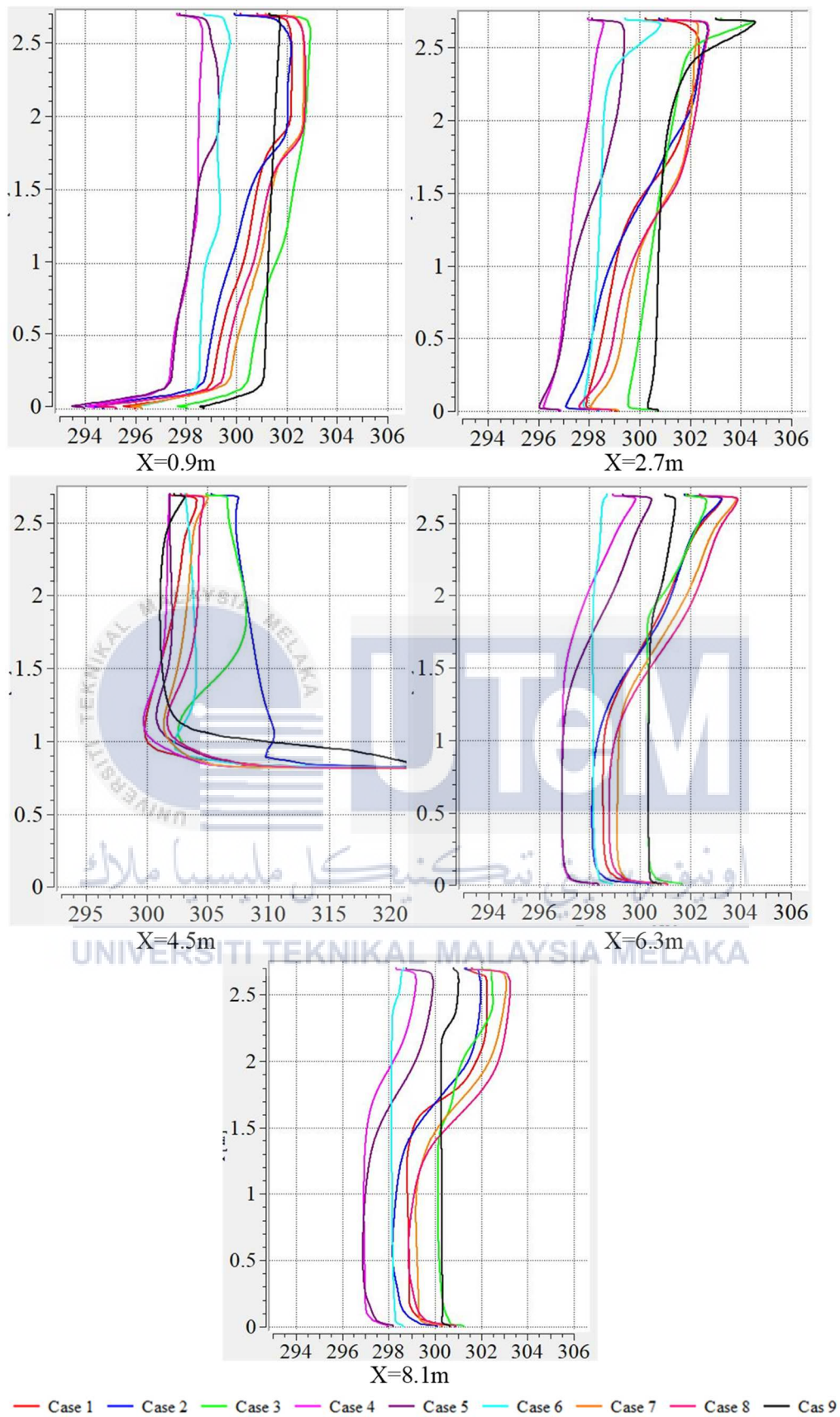
Figure 4.12: Graph of Vertical height Z, m against room air temperature, K for all cases on

symmetry plane at X= 0.9m, 2.7m, 4.5m, 6.3m and 8.1m
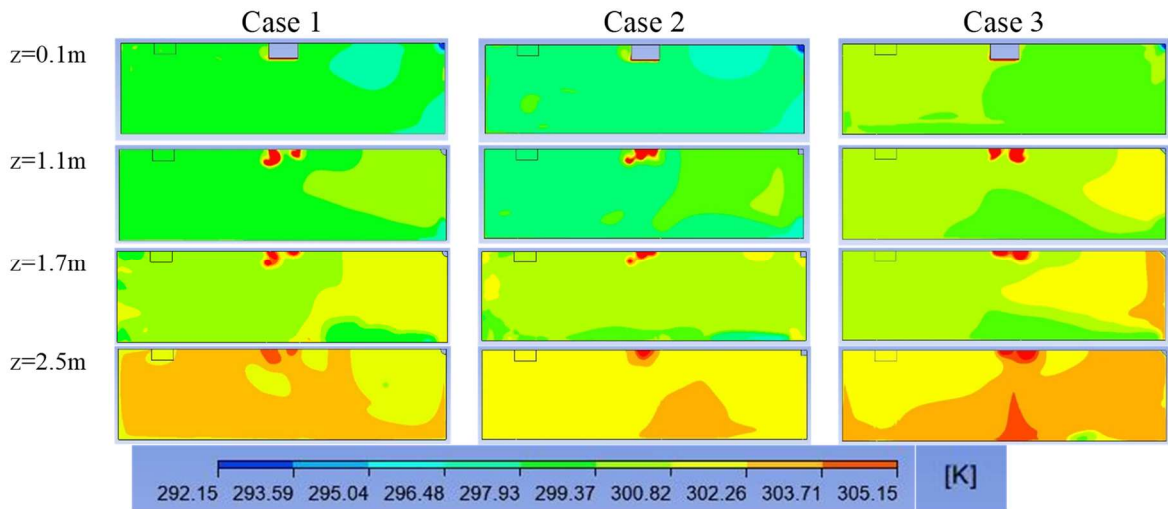
Figure 4.13: Temperature distribution (top view) for Case 1, Case 2 and Case 3 at vertical level from feet to head (sedentary and standing) and ceiling vicinity.
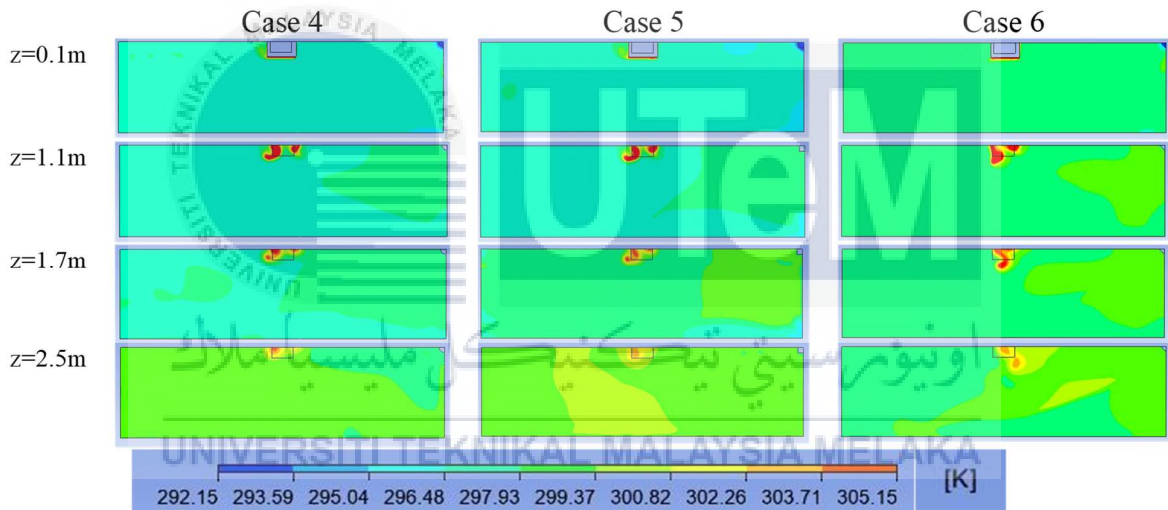
Figure 4.14: Temperature distribution (top view) for Case 4, Case 5 and Case 6 at vertical level from feet to head (sedentary and standing) and ceiling vicinity.

47
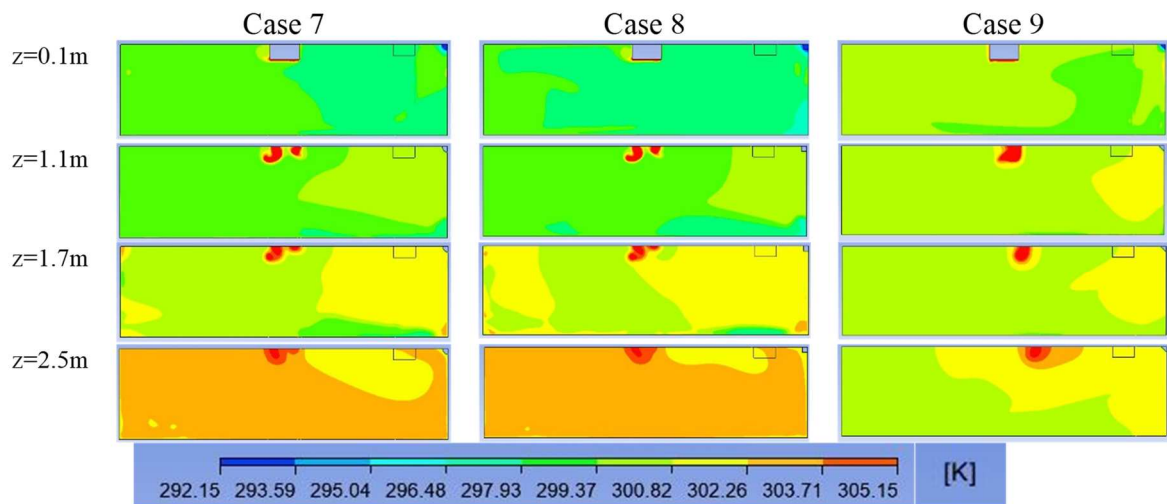
Figure 4.15: Temperature distribution (top view) for Case 7, Case 8 and Case 9 at vertical level from feet to head (sedentary and standing) and ceiling vicinity.

Not like the trend in velocity field comparison, the temperature difference between different shape of inlet is more obvious near the floor and becomes less significant at the ceiling level (Figure 4.13, 4.14, 4.15).

From Figure 4.13, 4.14 and 4.15, it can be seen that the temperature distribution Figure for Case 4, 5 and 6 are mostly dominate by light blue to green contour ($23^{o}C$ - $26^{o}C$) from floor level until ceiling vicinity while Case 1, 2, 3, 7, 8 and 9 are mostly dominate by yellow and orange color contour ($26\ ^{o}C$ – $30\ ^{o}C$) at $z = 1.7$ m and 2.5 m. This means that the for the room with exhaust placing at the middle can provide a colder environment compare to other cases. This statement is further proved in the Table 4.2.

Based on the Table 4.2, it can be known that the average temperature difference for all cases at $z = 1.7$ m and $z = 2.5$ m are around 1 ^{o}C to 2 ^{o}C while the temperature difference at $z = 0.1$ m and $z = 1.1$ m are only around 1 ^{o}C. Besides that, the average temperature difference between the cases for the exhaust located at the middle with others cases exhaust located at upwind and downwind can up to 3 ^{o}C while the in term of comparing the shape of inlet the temperature difference within 3 types of inlet nozzle only shows a 0.5 ^{o}C to 1 ^{o}C throughout the whole domain.

48

Table 4.2: Average Temperature value on each plane at vertical level from feet to head (sedentary and standing) and ceiling vicinity

Temperature, ºC				
Z (m)	0.1	1.1	1.7	2.5
Case 1	25.419	26.240	27.422	29.372
Case 2	24.972	25.864	27.532	29.291
Case 3	26.890	27.533	28.015	29.851
Case 4	23.788	24.289	24.604	26.067
Case 5	23.817	24.387	25.267	26.777
Case 6	25.040	25.421	25.483	25.942
Case 7	25.953	26.873	28.054	29.923
Case 8	23.636	26.627	28.441	30.107
Case 9	27.227	27.732	27.809	29.369

Based on the ICOP on IAQ 2010 which has been discuss in section 2.1.2, the acceptable range for the indoor air temperature in a building are within 23 ºC to 26 ºC. From the Table 4.2, it can be notice that Case 4 comply to this standard at all plane; Case 5 and 6 are comply to this standard from ankle level (z=0.1 m) until standing level (z=1.7 m); Case 1 and 2 comply at plane z = 0.1 m and z =1.1 m; Case 7 and 8 only comply at plane z = 0.1 m and Case 3 and 9 are not comply to this standard.

Lastly the vertical air temperature difference from ankle (0.1 m) to head (1.7 m) level (Figure 4.16) is calculated by using the data in Table 4.2. Based on the ASHRAE standard the vertical air temperature difference should be less than 3 °C in order to provide comfort environment to all of the occupants inside the room. In the Figure 4.16, it can be seen that most of the case are comply to the ASHRAE standard (ASHRAE 55-2004) while only Case 8 shows a huge increase in vertical temperature and exceed the acceptable range.
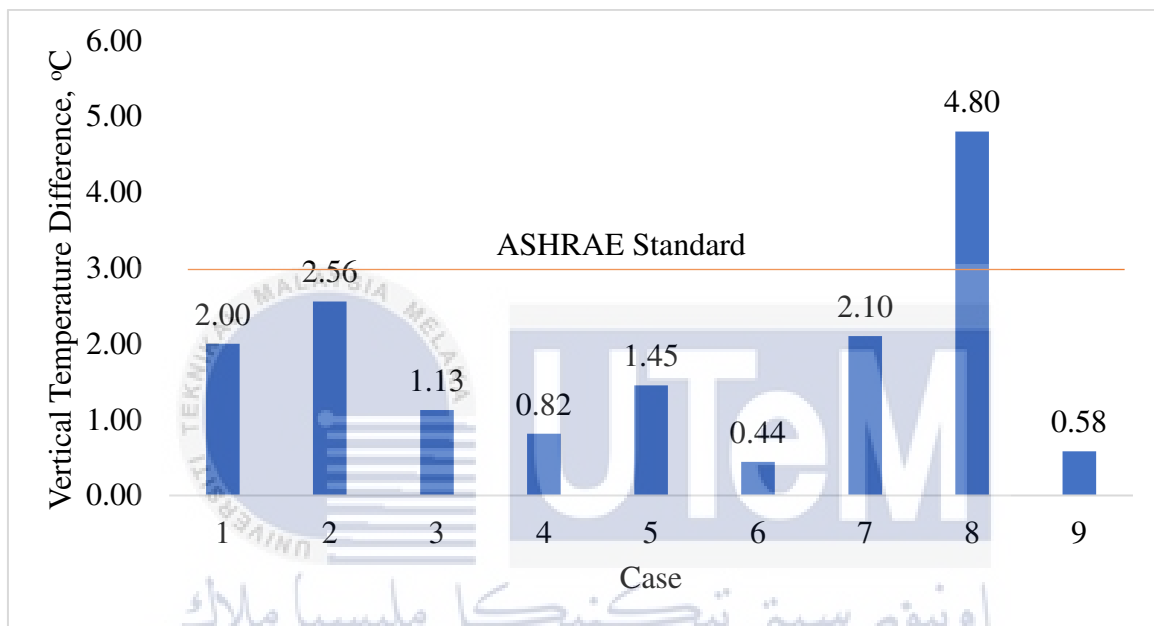

Figure 4.16: Vertical Temperature Difference between plane 0.1m and 1.7m for each case

4.3   Ventilation Criteria

In this section, the discuss will continue on some ventilation criteria which are always need to take account to when doing research for ventilation system. These criteria are Draught rate/ Draft (DR) and Percentage dissatisfied (PD) which had been discuss on Section 2.3.1.

4.3.1   Draught rate/ Draft (DR)

Based on the draught rate equation (2.1) stated in section 2.3.1, the draft in each case is calculated and presented in Figure 4.17. The mean air velocity and local air temperature are using the data in Table 4.1 (mean air velocity) and 4.2 (local air temperature) while the local turbulence intensity based on the graph in Figure 2.7.

From Figure 4.17 it can be notice that the turbulence intensity for all the cases at 0.1m is far higher than 1.1 m and 1.7 m. Most of the cases shown are comply to the acceptable draught rate which is smaller than 20% by ASHRAE standard (ASHRAE 55-2004) while only Case 6 exceed the acceptable range. The 0% draught rate at z = 1.7 m on case 2 and case 8 is due to the mean air velocity at that selected plane is below 0.05 m/s. Hence according to the description in the formula, if the measured mean air velocity is below 0.05 m/s, 0.05 m/s is taken instead of the measured value. Thus by inserting 0.05 m/s as mean air velocity into the equation will resulting getting a 0% draught rate which means that the draught rate at the targeted location is insignificant.
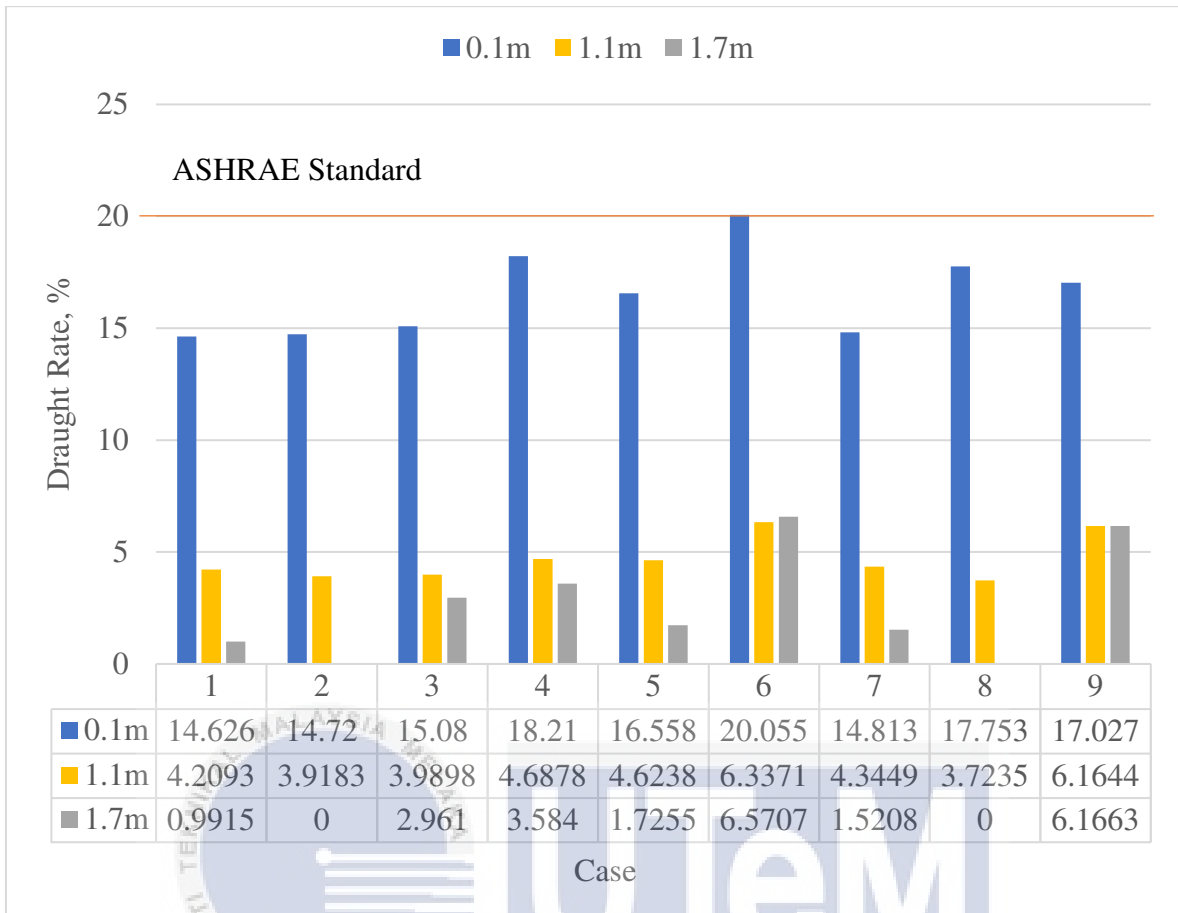
Figure 4.17: Draught Rate at Z = 0.1m, 1.1m, 1.7m

4.3.2 Percentage dissatisfied (PD)

Based on the Percentage dissatisfied (PD) equation (2.2) stated in section 2.3.1, the PD for each case is calculated and presented in Figure 4.17. The value for $\Delta T_{0.1-1.1}$ is obtained by calculate the temperature difference between plane z = 0.1 m and z = 1.1 m and the graph of PD for each case is shown in Figure 4.18.

From Figure 4.18, it can be seen that the PD value for most of the cases is within 0.4% to 0.7% while only Case 8 shown a 3.92%. Although based on the ASHRAE standard (ASHRAE 55-2004) any PD value due to vertical air temperature difference below 5% is under acceptable range and all of the case is comply to this standard but it can be known that Case 8 is under a more local discomfort environment when comparing to other cases.

Figure 4.18: Percentage Dissatisfied

4.4   Summary

In a nutshell, position of exhaust will cause a larger impact toward the indoor thermal environment when comparing to the shape of inlet nozzle while in terms of velocity field the shape of inlet nozzle is more influential when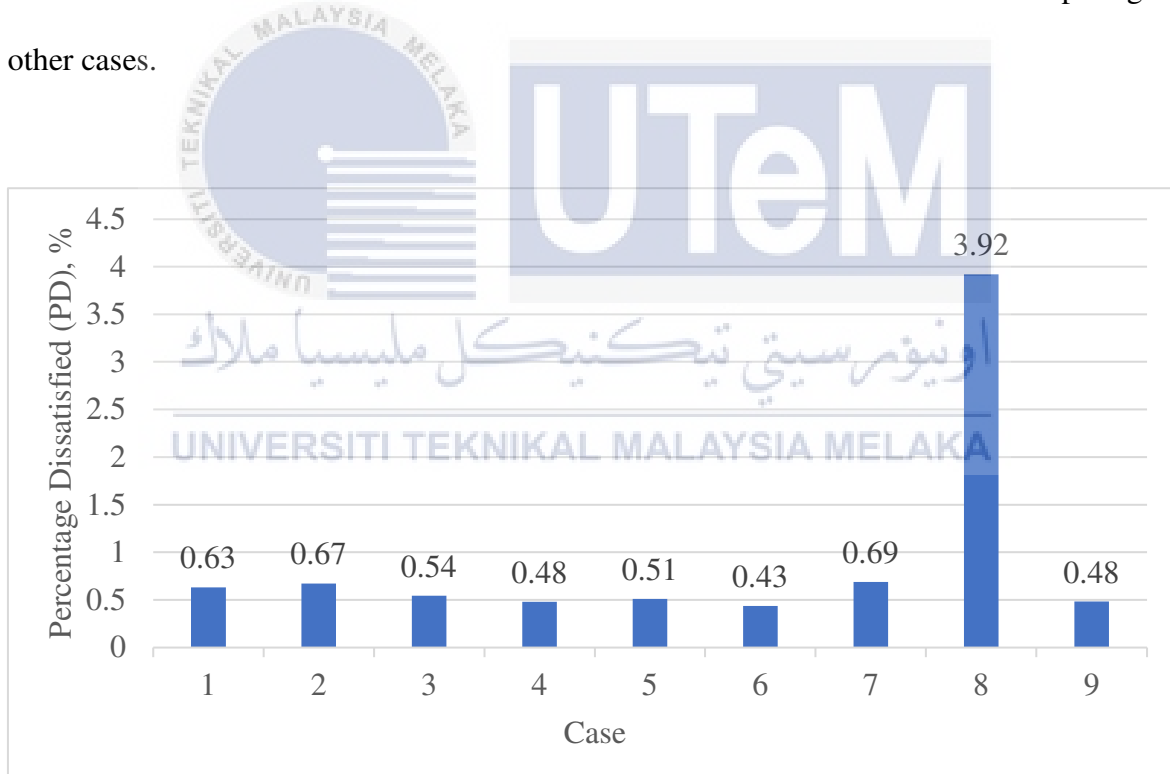 comparing to position of exhaust. From the result obtained, Case 4 is the case with the best indoor air quality among all 9 cases. Case 4 obtained a 0.82 ºC in vertical temperature difference analysis; 3.584% at Z=0.1 m, 4.6878% in Z=1.1 m, 18.21% at Z=1.7 m for draught rate and 0.48% percentage dissatisfied due to vertical air temperature difference. Although Case 4 shows an ordinary result in the draught rate graph (Figure 4.17) and the average air velocity from each vertical plane have a small difference with the acceptable room temperature stated in ICOP, but it performs well in the percentage dissatisfied graph (Figure 4.18) and also vertical temperature difference graph (Figure 4.18). Besides that, Case 4 is also the only case where the average temperature for all vertical plane investigated are comply to the acceptable indoor air temperature stated in ICOP while other cases are not fully comply to it.
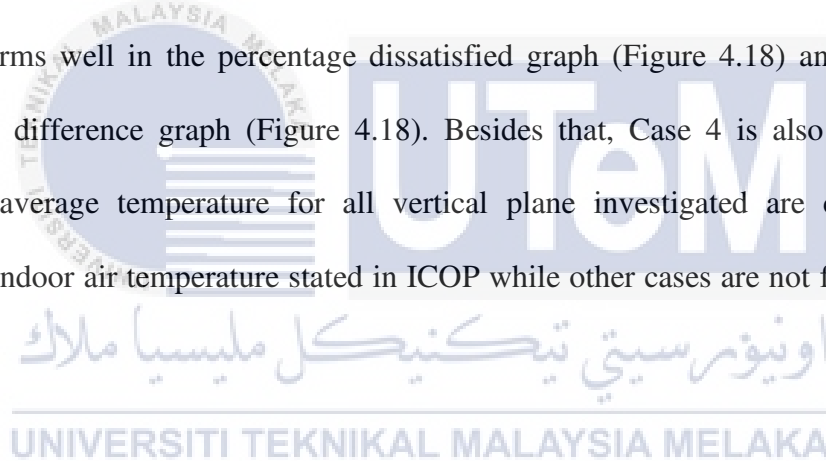
CHAPTER 5

CONCLUSION AND RECOMMENDATION FOR FUTURE RESEARCH

5.1   Conclusion

In this final year project, a ventilation strategy called Impinging Jet Ventilation (IJV) has been discuss and investigated as a possible solution to thermal comfort and IAQ. In order to study the effects of IJV towards the thermal condition inside a closed room, two objectives have been proposed and then examined. These objectives are achieved throughout the study in this project where objective 1 is achieved in chapter 3 and objective 2 is achieved in chapter 4.

For objective 1, a full scale laboratory office equip with IJV system is designed by using SOLIDWORKS. The dimension of this model is based on the article published by Kobayashi, Sugita, Umemiya, Kishimoto & Sandberg (2017). After the model is validated, the position of the exhaust and also the shape of the inlet is modified in order to achieve the evaluating criteria in objective 2 where the combination of the position of exhaust and the shape of inlet are described in Table 3.1.

Next for objective 2, the velocity profile and temperature field for each case are presented and investigated. The results shows that position of exhaust bring a larger effect toward the velocity and temperature field inside the room compare to the difference in the shape of inlet. The discussion found out that Case 4 can provide the best indoor thermal environment where Case 4 performs well in the PD, also vertical temperature difference and room average temperature while Case 8 provide the worst scenario.

5.2   Recommendation for future research

Considering the further studies in the impinging jet ventilation system, there are a few suggestions are provided here in order to create a more efficient impinging jet ventilation system which can provide a more comfortable indoor environment to user. Firstly, the investigation of relationship between the height of inlet nozzle and the thermal environment of a targeted space can be carry out. This can help to understand more on the characteristic of impinging jet ventilation system.

Next, the study of the effects on having both impinging jet ventilation system and air conditioning system inside a targeted space can be carry out. This can help to investigate did the IAQ, thermal environment and also energy consumption become more better when having both system inside a single room compare to only having one of those.

While for the computational fluid dynamics (CFD) simulation, it is recommended that the simulation run with ACT extension for thermal comfort so that the contour plots for mean age of air, PMV and PPD can be generate in the result tab. Besides that, the simulation can change into transient flow so that the condition of the flow from initial until steady state can be seen.

REFERENCE

A. A. Mahdi and S. M. Abbas, "Experimental and Theoretical Investigation of Impinging Jet Ventilation at Different Cross Sectional Area of Supply Air Duct", *JUBES*, vol. 26, no. 5, pp. 238 - 257, Mar. 2018.

Ameen, A., Cehlin, M., Larsson, U., & Karimipanah, T. (2019). Experimental Investigation of the Ventilation Performance of Different Air Distribution Systems in an Office Environment—Cooling Mode. *Energies*, *12*(7), 1354.

Amirhosein Ghaffarianhoseini, Husam AlWaer, Hossein Omrany, Ali Ghaffarianhoseini, Chaham Alalouch, Derek Clements-Croome & John Tookey. (2018, May 2). *Sick building syndrome: are we doing enough?*

Anne Steinemann, Pawel Wargocki & Behzad Rismanchi. (2017, February 1). *Ten questions concerning green buildings and indoor air quality*. ScienceDirect.

Awbi, H. B. (2015). *Ventilation and Air Distribution Systems in Buildings*. Frontiers.

Balakrishnan, P., & Srinivasan, K. (2019). Impinging jet noise reduction using non-circular jets. *Applied Acoustics*, *143*, 19–30.

Barták, M., Cermák, M., Clarke, J., Denev, J., Drkal, F., Lain, M., Macdonald, I., Majer, M., & Stankov, P. (2001 August 13). *Experimental and numerical study of local mean age of air.*

Carrie A Redlich, Judy Sparer, Mark R Cullen. (1997, April 5). *Sick-building syndrome*. ScienceDirect.

Chen, H. J., Moshfegh, B., & Cehlin, M. (2012). Numerical investigation of the flow behavior of an isothermal impinging jet in a room. *Building and Environment*, *49*, 154–166.

Chung-Yen Lu, Meng-Chuan Tsai, Chih-Hsin Muo, Yu-Hsien Kuo, Fung-Chang Sung & Chin-Ching Wu. (2017, November 20). *Personal, Psychosocial and Environmental Factors Related to Sick Building Syndrome in Official Employees of Taiwan.*

Federspiel, C. C. (1999). Air-Change Effectiveness: Theory and Calculation Methods. *Indoor Air*, *9*(1), 47–56.

G.J. Poitras, A. Babineau, G. Roy & L.-E. Brizzi. (2017, April 1). *Aerodynamic and heat transfer analysis of a impinging jet on a concave surface.*ScienceDirect.

Guodong Ye, Changzhi Yang, Youming Chen & Yuguo Lib. (2003) *A new approachfor measuring predicted mean vote (PMV) and standard effective temperature (SET*).*

Haghshenaskashani, S., Sajadi, B., & Cehlin, M. (2018, May 16). *Multi-objective optimization of impinging jet ventilation systems: Taguchi-based CFD method.* Building Simulation.

Idris, N. F. B. (2010). *Official Website Department of Occupational Safety and Health - Indoor Air Quality.* Official Website Department of Occupational Safety and Health.

Ifa, S., & Driss, Z. (2020, September 4). *Numerical simulation and experimental validation of the ventilation system performance in a heated room.* Air Quality, Atmosphere & Health.

INDUSTRY CODE OF PRACTICE ON INDOOR AIR QUALITY 2010 DEPARTMENT. (2010). Department Of Occupational Safety And Health Ministry Of Human Resources, Malaysia.

Jambunathan, K., Lai, E., Moss, M. A., & Button, B. L. (1992). A review of heat transfer data for single circular jet impingement. *International Journal of Heat and Fluid Flow*, *13*(2), 106–115.

Julia Wienand, Andris Riedelsheimer, Bernhard Weigand. (2017, January 1). *Numerical study of a turbulent impinging jet for different jet-to-plate distances using two-equation turbulence models*. ScienceDirect.

Karimipanah, T., & Awbi, H. B. (2002). Theoretical and experimental investigation of impinging jet ventilation and comparison with wall displacement ventilation. *Building and Environment*, *37*(12), 1329–1342.

Kobayashi, T., Nishiumi, T., & Umemiya, N. (2019). Simplified Prediction Method of Vertical Temperature Distribution for Impinging Jet Ventilation System. *E3S Web of Conferences*, *111*, 01097.

Kobayashi, T., Sugita, K., Umemiya, N., Kishimoto, T., & Sandberg, M. (2017). Numerical investigation and accuracy verification of indoor environment for an impinging jet ventilated room using computational fluid dynamics. *Building and Environment*, *115*, 251–268.

Naseem Uddina, Bernhard Weigand & Bassam A. Younis. (2019, January 1). *Comparative study on heat transfer enhancement by turbulent impinging jet under conditions of swirl, active excitations and passive excitations*. ScienceDirect.

Nuntadusit, C., Wae-hayee, M., & Kaewchoothong, N. (2018). Heat transfer enhancement on a surface of impinging jet by increasing entrainment using air-augmented duct. *International Journal of Heat and Mass Transfer*, *127*, 751–767.

Qin, C., & Lu, W.-Z. (2020). Effects of ceiling exhaust location on thermal comfort and age of air in room under impinging jet supply scheme. *Journal of Building Engineering*, 101966.

Samira Haghshenaskashani, Behrang Sajadi. (2018, July 1). *Evaluation of thermal comfort, IAQ and energy consumption in an impinging jet ventilation (IJV) system with/without ceiling exhaust*. ScienceDirect.

Shouhong Ren, Shuo Tian & Xiangyi Meng. (2015, January 1). *Comparison of Displacement Ventilation, Mixing Ventilation and Underfloor Air Distribution System.* Researchgate.

Sun, B., Qu, Y., & Yang, D. (2016). Heat transfer of Single Impinging Jet with Cu Nanofluids. Applied Thermal Engineering, 102, 701–707.

Surendra D. Barewar, Shravan Tawri, Sandesh S. Chougule. (2019, February 1). *Heat transfer characteristics of free nanofluid impinging jet on flat surface with different jet to plate distance: An experimental investigation*. ScienceDirect.

Wae-hayee, M., Yeranee, K., Piya, I., Rao, Y., & Nuntadusit, C. (2019). Heat transfer correlation of impinging jet array from pipe nozzle under fully developed flow. *Applied Thermal Engineering*, *154*, 37–45.

Xiao Ye, Yanming Kang, Xiufeng Yang & Ke Zhong. (2018, January 1). *Temperature distribution and energy consumption in impinging jet and mixing ventilation heating rooms with intermittent cold outside air invasion*. ScienceDirect.

Xiao Ye, Yanming Kang, Zhenrong Yan, Bin Chen& Ke Zhong (2019, August 1). *Comparison study of contaminant distribution and indoor air quality in large-height spaces between impinging jet and mixing ventilation systems in heating mode*. ScienceDirect.

Xiao Ye, Yanming Kang, Zhenrong Yan, Bin Chen& Ke Zhong. (2020, June 15). *Optimization study of return vent height for an impinging jet ventilation system with exhaust/return-split configuration by TOPSIS method*. ScienceDirect.

Xinyue Huo, Yuexia Sun, Jing Hou, Pan Wang, Xiangrui Kong, Qingnan Zhang, Jan Sundell. (2020, February 1). *Sick building syndrome symptoms among young parents in Chinese homes*. ScienceDirect.

Yang, X., Ye, X., Zuo, B., Zhong, K., & Kang, Y. (2020, September 21). *Analysis of the factors influencing the airflow behavior in an impinging jet ventilation room*. Building Simulation.

Yao, S., Guo, Y., Jiang, N., & Liu, J. (2015). Experimental investigation of the flow behavior of an isothermal impinging jet in a closed cabin. *Building and Environment*, *84*, 238–250.

Ye, X., Zhu, H., Kang, Y., & Zhong, K. (2016). Heating energy consumption of impinging jet ventilation and mixing ventilation in large-height spaces: A comparison study. *Energy and Buildings*, *130*, 697–708.